AD

MEMORANDUM REPORT ARBRL-MR-02991

SUPERSONIC WIND TUNNEL MEASUREMENTS OF STATIC AND MAGNUS AERODYNAMIC COEFFICIENTS FOR PROJECTILE SHAPES WITH TANGENT AND SECANT OGIVE NOSES

Charles J. Nietubicz
Klaus O. Opalka

February 1980

US ARMY ARMAMENT RESEARCH AND DEVELOPMENT COMMAND
BALLISTIC RESEARCH LABORATORY
ABERDEEN PROVING GROUND, MARYLAND

Destroy this report when it is no longer needed.
Do not return it to the originator.

Secondary distribution of this report by originating or sponsoring activity is prohibited.

Additional copies of this report may be obtained from the National Technical Information Service, U.S. Department of Commerce, Springfield, Virginia 22151.

The findings in this report are not to be construed as an official Department of the Army position, unless so designated by other authorized documents.

The use of trade names or manufacturers' names in this report does not constitute indorsement of any commercial product.

UNCLASSIFIED

SECURITY CLASSIFICATION OF THIS PAGE *(When Date Entered)*

REPORT DOCUMENTATION PAGE		READ INSTRUCTIONS BEFORE COMPLETING FORM
1. REPORT NUMBER MEMORANDUM REPORT ARBRL-MR-02991	2. GOVT ACCESSION NO.	3. RECIPIENT'S CATALOG NUMBER
4. TITLE *(and Subtitle)* SUPERSONIC WIND TUNNEL MEASUREMENTS OF STATIC AND MAGNUS AERODYNAMIC COEFFICIENTS FOR PROJECTILE SHAPES WITH TANGENT AND SECANT OGIVE NOSES		5. TYPE OF REPORT & PERIOD COVERED Final 6. PERFORMING ORG. REPORT NUMBER
7. AUTHOR(s) Charles J. Nietubicz Klaus O. Opalka		8. CONTRACT OR GRANT NUMBER(s)
9. PERFORMING ORGANIZATION NAME AND ADDRESS U.S. Army Ballistic Research Laboratory (ATTN: DRDAR-BLL) Aberdeen Proving Ground, Maryland 21005		10. PROGRAM ELEMENT, PROJECT, TASK AREA & WORK UNIT NUMBERS RDT&E 1L662618AH80
11. CONTROLLING OFFICE NAME AND ADDRESS U.S. Army Armament Research & Development Command U.S. Army Ballistic Research Laboratory (ATTN: DRDAR-BL) Aberdeen Proving Ground, MD 21005		12. REPORT DATE FEBRUARY 1980 13. NUMBER OF PAGES 73
14. MONITORING AGENCY NAME & ADDRESS*(if different from Controlling Office)*		15. SECURITY CLASS. *(of this report)* Unclassified 15a. DECLASSIFICATION/DOWNGRADING SCHEDULE

16. DISTRIBUTION STATEMENT *(of this Report)*

Approved for public release, distribution unlimited.

17. DISTRIBUTION STATEMENT *(of the abstract entered in Block 20, if different from Report)*

18. SUPPLEMENTARY NOTES

19. KEY WORDS *(Continue on reverse side if necessary and identify by block number)*

Aerodynamic coefficients, Magnus data, Supersonic wind tunnel tests, Bodies of Revolution.

20. ABSTRACT *(Continue on reverse side if necessary and identify by block number)*

Wind tunnel tests have been conducted for a series of projectile configurations. The shapes tested include a three caliber secant ogive nose and three caliber tangent ogive nose configuration. The overall model length was fixed at 6 calibers for all configurations tested. Static and Magnus aerodynamics coefficient data were obtained at Mach numbers 2.0, 3.0 and 4.0 for angles of attack up to 10.0°. The data are presented in graphical form along with tabulations of the summary data.

(continued)

DD FORM 1 JAN 73 1473 EDITION OF 1 NOV 65 IS OBSOLETE

UNCLASSIFIED

SECURITY CLASSIFICATION OF THIS PAGE *(When Date Entered)*

20. ABSTRACT. (continued)

The tangent ogive nose produced a slight increase in the Magnus moment coefficient when compared to similar secant ogive configurations. The boattail configuration, when compared to the cylinder shapes, were found to increase the Magnus moment, however, this effect was shown to decrease with increasing Mach number.

TABLE OF CONTENTS

LIST OF ILLUSTRATIONS

LIST OF TABLES

I. INTRODUCTION

A research effort to develop advanced numerical codes for computing aerodynamic forces acting on spinning slender bodies of revolution at angle of yaw is presently in progress at the Ballistic Research Laboratory. Computation of the Magnus force, which results from the combined high spin rate, and angle of yaw, is of particular interest. Experimental studies are being carried out in order to provide data for comparison to the numerical computations.[1,2,3] In this report, the results of a series of wind tunnel tests are reported in which measurements of pitch plane and Magnus effects have been measured for several slender bodies of revolution. A complete tabulation of the experimental data is provided in order to facilitate comparison to theoretical computations.

II. EXPERIMENTAL INVESTIGATION

A. Test Conditions

The wind tunnel test program was conducted for a series of ogive-cylinder-boattail shapes. The test was performed at free-stream Mach numbers, M_∞, of 2.0, 3.0, and 4.0. The models, with boundary-layer trip, were tested at angles of attack ranging from +10° to -4°. Magnus force was measured at spin rates, Pd/V, ranging from 0 to 0.4 at angles of attack, α, of 10°, 6°, 4°, 2°, 1°, 0, -2°, and -4°. The test conditions are summarized in Table I.

---

1. *W. B. Sturek, et al, "Computations of Turbulent Boundary Layer Development Over a Yawed, Spinning Body of Revolution With Application to the Magnus Effect," BRL Report No. 1985, May 1977, U.S. Army Ballistic Research Laboratory, Aberdeen Proving Ground, Maryland. AD A041338.*

2. *H. A. Dwyer, "Three Dimensional Flow Studies Over a Spinning Cone at Angle of Attack," BRL Contract Report No. 137, February 1974, U.S. Army Ballistic Research Laboratory, Aberdeen Proving Ground, Maryland. AD 774795.*

3. *H. A. Dwyer and B. R. Sanders, "Magnus Forces on Spinning Supersonic Cones. Part I: The Boundary Layer," BRL Contract Report No. 248, July 1975, U.S. Army Ballistic Research Laboratory, Aberdeen Proving Ground, Maryland. AD A013518. Also, AIAA Journal, Vol 14, No. 4, April 1976, p. 498.*

Table I. Test Conditions

Mach Number, M_∞	2.0	3.0	4.0
Supply Pressure, P_o			
mm Hg	1600	2250	3800
psia	30.79	43.30	73.12
MPa (MegaPascal)	.2123	.2985	.5041
Reynolds Number, $Re_\ell \times 10^{-6}$	8.505	7.317	7.425

B. Equipment

The Ballistic Research Laboratory Supersonic Wind Tunnel No. 1[4],* had a flexible, two-dimensional nozzle that was calibrated for fifteen Mach numbers between 1.5 and 5.0 with an accuracy of 0.01 absolute value. The air density could be varied to cover a Reynolds number range from 4×10^6 to 30×10^6 per meter. The supply pressure was variable from 0.033 MPa to 6.67 MPa (MegaPascal) in continuous operation. (NOTE: 1 atm ≡ 0.101325 MPa). The test section measured 381 mm high and 330 mm wide, and allowed testing of models of 50 mm diameter and 250 mm length at the most critical Mach number of 1.50. The angle of attack range was from -10 to +15 degrees.

C. Model Details

The basic model tested was an ogive-cylinder-boattail. The configurations for which data have been obtained are:

4. *J. C. McMullen, "Wind Tunnel Testing Facilities at the Ballistic Research Laboratories," BRL Memorandum Report No. 1292, July 1960, U.S. Army Ballistic Research Laboratory, Aberdeen Proving Ground, Maryland. AD 244180.*

* *The BRL Wind Tunnel Facilities are no longer operational.*

TABLE II. MODEL CONFIGURATIONS

Model Description	Configuration Number
Secant-Ogive-Cylinder (SOC)	1.0
Secant-Ogive-Cylinder With Boattail (SOCBT)	3.0
Tangent-Ogive-Cylinder (TOC)	5.0
Tangent-Ogive-Cylinder With Boattail (TOCBT)	7.0

Both the secant and tangent ogive nose are 3 calibers in length. The cylinder section is 3 calibers with the exception of the boattail configuration. When the 1 caliber 7.0° boattail is added the cylinder length is shortened to 2 calibers, thus, always maintaining a 6 caliber total length model.

The reference diameter is 57.15 mm (2¼ inches). The radius of the secant ogive and tangent ogive is 1079.0 mm (42.48 inches) and 528.86 mm, respectively. A mechanical boundary-layer trip was installed on the ogive 40.6 mm (1.60 inches) from the nose. It consists of three contoured rings of 1.52 mm width per ring. The height of the trip is 0.508 mm. The general dimensions of the two basic models are given in Figure 1.

The outer shell of the model is free to rotate about its longitudinal axis by means of two ball bearing mounts. The inner races of the ball bearings are mounted on a non-rotating sleeve that fits over the free end of the balance-strut assembly. The model is driven by an air turbine which is installed on the strut behind the balance. The air leaving the turbine blows against a ring of turbine blades which are installed at the base of the model shell, and causes the model to rotate.

The model is mounted on the free end of the balance-strut assembly which forms a cantilevered beam with the wind tunnel angle of attack system. The aerodynamic forces acting on the model are transmitted through the balance into the wind tunnel structure. A six-component, strain-gage balance was used to measure the aerodynamic forces and moments. The balance has the following capacities (with references to the balance center located between gages).

Normal Force	180 N	Pitching Moment	5.20 N•m
Side Force	90 N	Yawing Moment	2.60 N•m
Axial Force	90 N	Roll Moment	2.26 N•m

The distance between forward and rear gages measures 58.42 mm.

The model underwent a static-force (polar) test without spin. The angle of attack was varied from +10° to -4°. A sample reading was taken automatically by the Data Acquisition System[5] every two seconds, which corresponds to an approximate change of 0.25 degree in angle of attack.

Additionally, the model was subjected to a spin test to measure the Magnus force and the Magnus moment. Data were obtained for all runs over a spin range of 30,000 RPM. The model was spun up to 35,000 RPM and data were taken while the model was coasting down in spin rate.

III. RESULTS

A. Data Reduction

The raw data were reduced to coefficient form on the BRL computer using our standard program. The angles of attack were corrected for strut deflections due to aerodynamic loads and for the flow inclination in the wind tunnel. The derivatives of the normal force and of the pitching moment near zero angle of attack were obtained from a linear regression of eleven test points in the α-range from -1.5 to +1.5 degrees.

A translational correction was applied to the side-force and yawing-moment data such that all curves would pass through the origin of the graph.

B. Data Presentation

The reduced static force data are presented in non-dimensional form and include plots of C_N, C_M, and C_A versus angle of attack. These basic plots are located in the Appendix which is divided into two sections. Appendix A contains data for the SOC and SOCBT configuration while Appendix B contains the TOC and TOCBT data.

The aerodynamic coefficient data are presented in tabular form in Tables III, IV and V, VI for the Secant-Ogive and Tangent-Ogive configuration respectively. These tabulations include the normal force

---

5. *L. D. Kayser, "The BRL Wind Tunnel High Speed Analog to Digital Data Acquisition System," BRL Memorandum Report No. 2142, December 1971, U.S. Army Ballistic Research Laboratory, Aberdeen Proving Ground, Maryland. AD 737180.*

and pitching moment slopes (C_{N_α}, C_{M_α}), the Magnus force and moment coefficients (C_{N_p}, C_{M_p}) and the tunnel operating conditions.

C. Discussion

A linear fit, of the side force and yawing moment data over the full spin range, was performed for the SOC and SOCBT configurations. The resultant slopes (C_{N_p}, C_{M_p}) are tabulated in Table IV. Additionally, similar fits were performed for the TOC and TOCBT configurations with the exception that the range of fit was limited to $Pd/V \leq .20$. These data are found in Table VI.

Summary plots were developed to show the variation in Magnus moment coefficient for changes in ogive shape, Mach number, and the addition of a boattail as a function of angle of attack. The moment was referenced to a point located at 63% of the model length as measured from the nose.

Figure 2 shows the Mach number effect on C_{M_p} for the SOCBT configuration. The decrease in Magnus moment with increasing Mach number is typical of all configurations tested. The increase in the Magnus moment due to the addition of the boattail can be seen in Figure 3 at M = 2. However, as the Mach number increases (Figures 4 and 5) the difference in the Magnus moment between the SOC and SOCBT shapes becomes less. This is also true for the TOC and TOCBT configurations.

A change in the nose shape from a secant to a tangent ogive is found to produce an increase in the Magnus moment coefficient as shown in Figure 6 for M = 2 and Figure 7 for M = 3.

As a final analysis of the data, a linear fit of the Magnus moment data was performed for an angle of attack range of -3° to +3°. The resultant plot is shown in Figure 8 for the SOC and SOCBT configuration. The Magnus moment slope is shown to decrease with increasing Mach number; the boattail effect is also shown to be less apparent with increasing Mach number.

D. Conclusions

A series of wind tunnel tests have been run for models with secant and tangent ogives and having cylindrical and boattailed afterbodies. The tests were conducted at M = 2, 3 and 4 to determine both pitch plane and Magnus aerodynamic coefficient data. A summary of the findings of this study indicate:

(1) $C_{M_{p_\alpha}}$ decreases with increasing Mach number for all configurations.

(2) Boattail configurations increased the Magnus moment coefficient at M = 2.0. The difference at M = 3 and 4 was negligible.

(3) The effect of the tangent ogive is to increase the Magnus moment when compared to similar secant-ogive configurations.

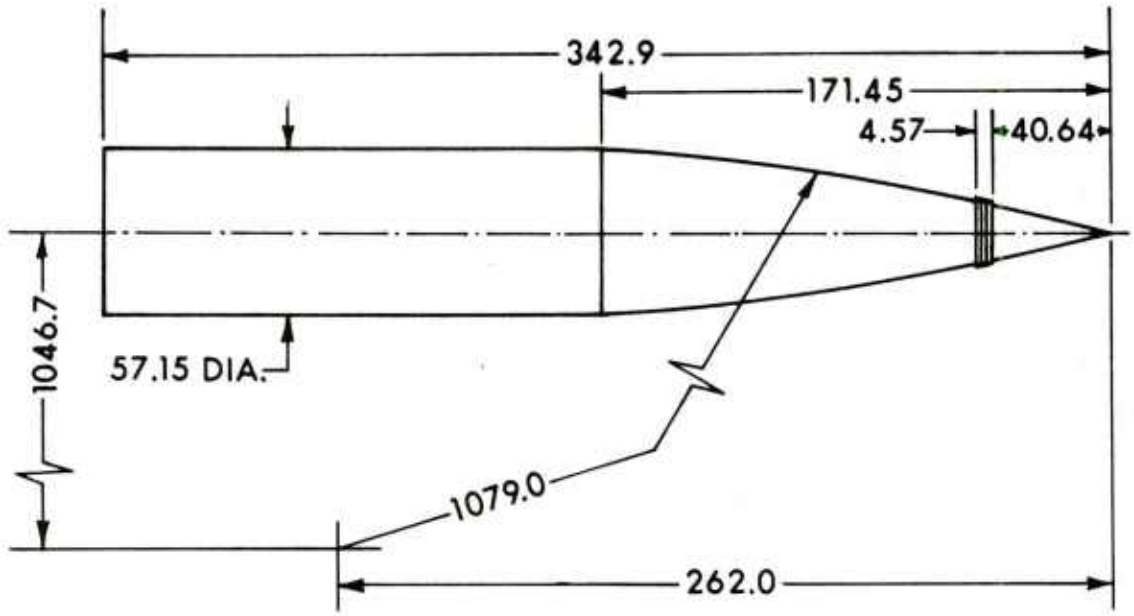

Configuration 1.0. Secant-Ogive-Cylinder

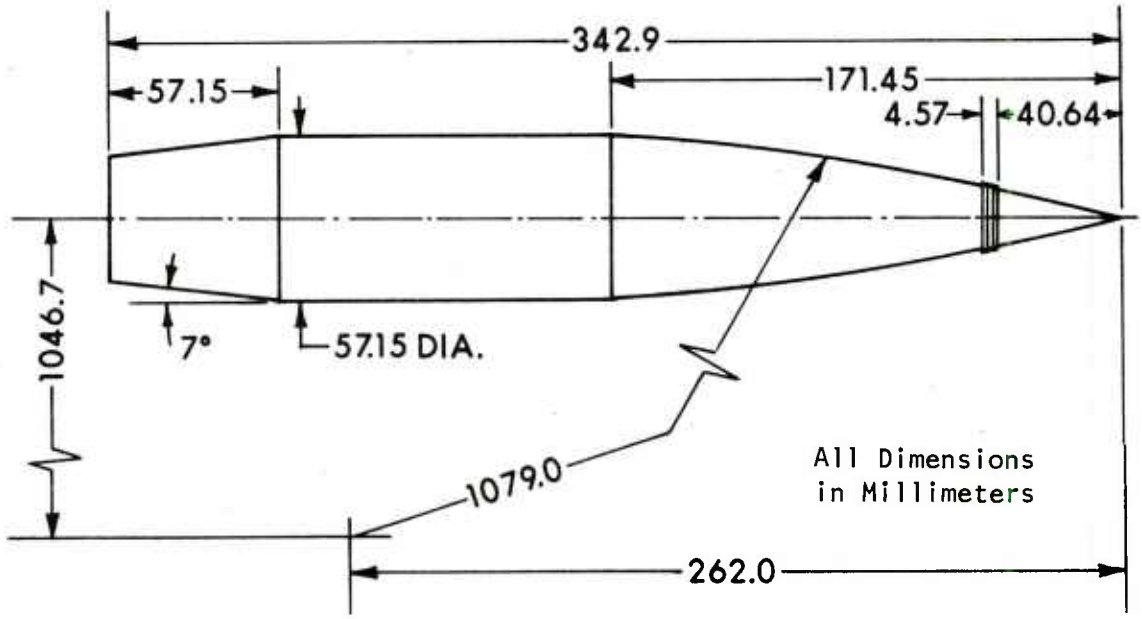

Configuration 3.0. Secant-Ogive-Cylinder with Boattail

Figure 1. Model Details

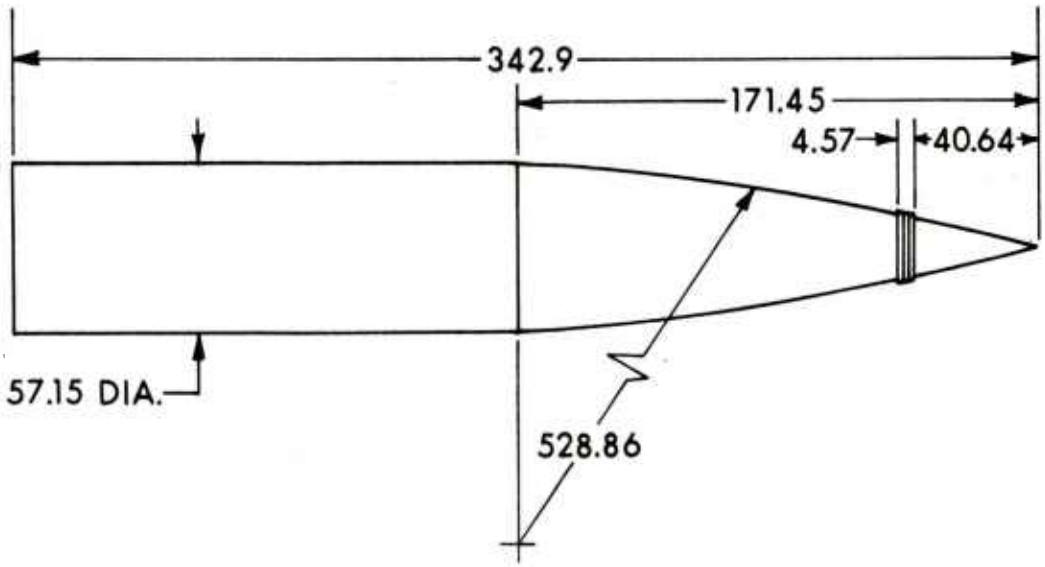

Configuration 5.0. Tangent-Ogive-Cylinder

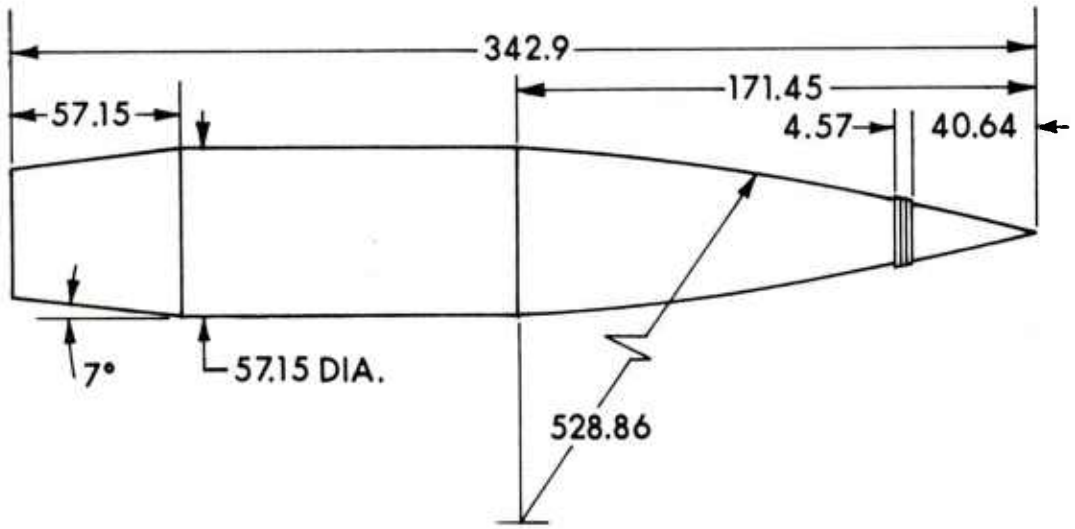

Configuration 7.0. Tangent-Ogive-Cylinder with Boattail

Figure 1. Continued

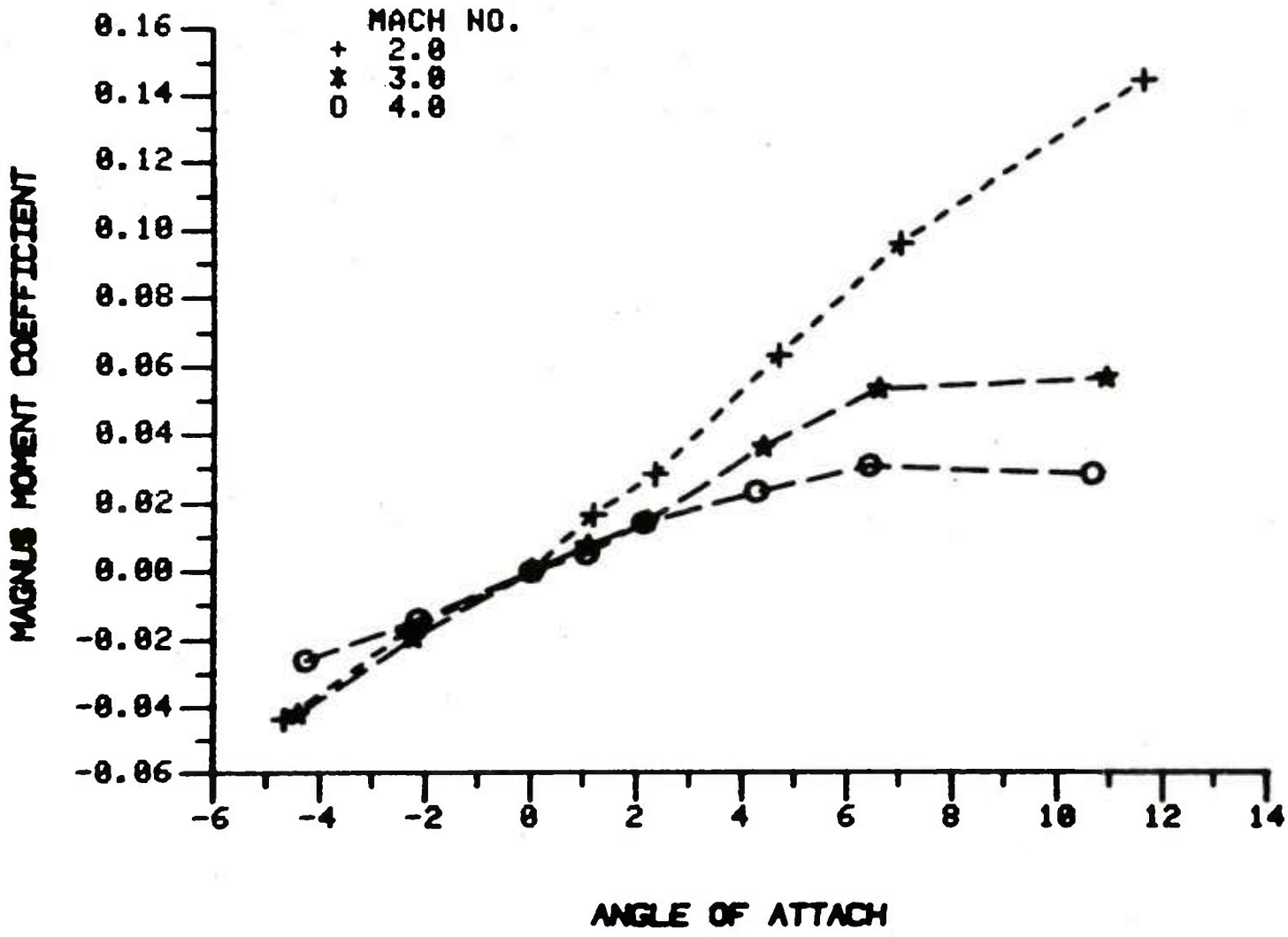

Figure 2. Mach Number Effect on Magnus Moment Coefficient, Secant-Ogive-Cylinder with Boattail

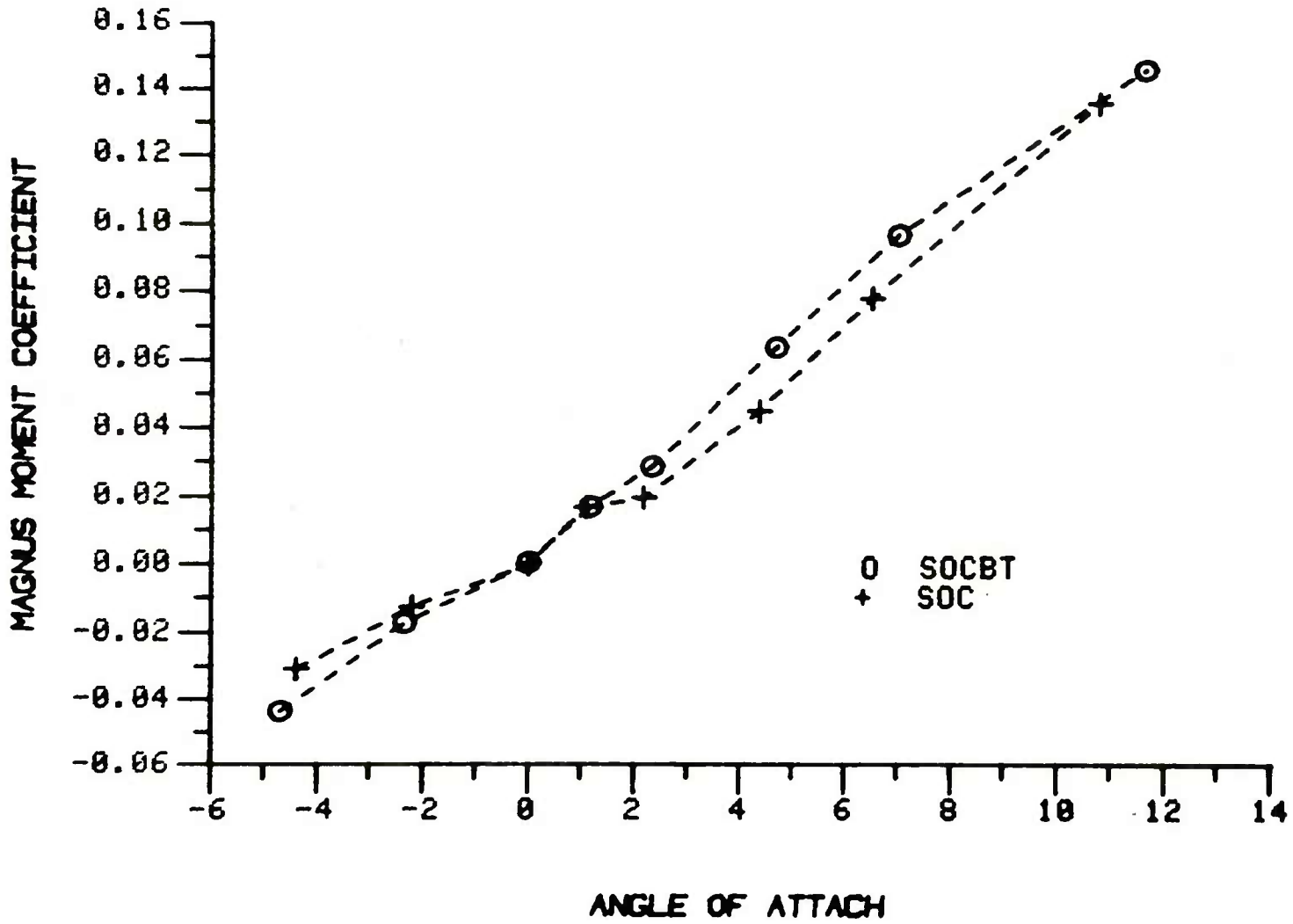

Figure 3. Boattail Effect on Magnus Moment Coefficient, M = 2.0

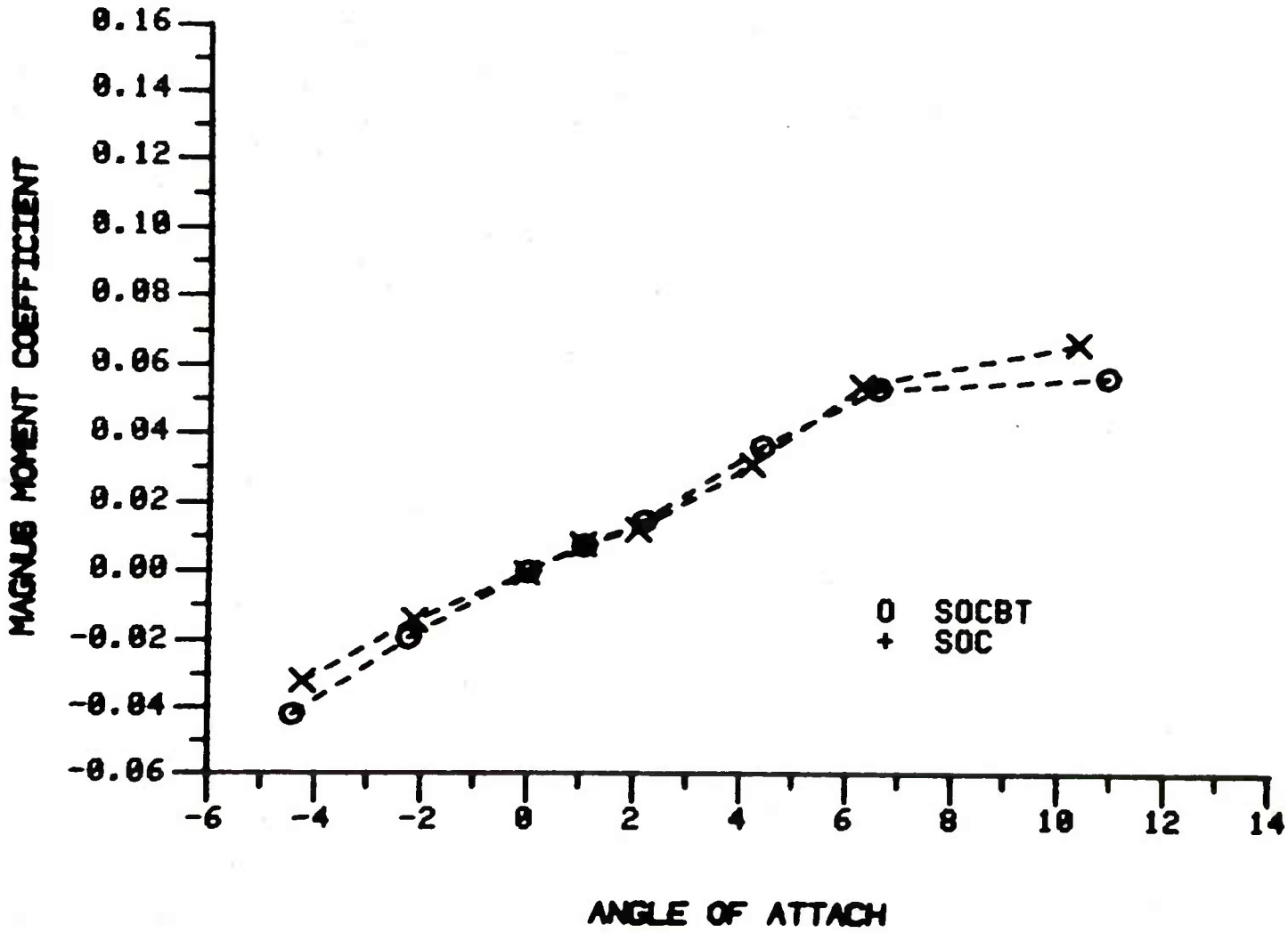

Figure 4. Boattail Effect on Magnus Moment Coefficient, M = 3.0

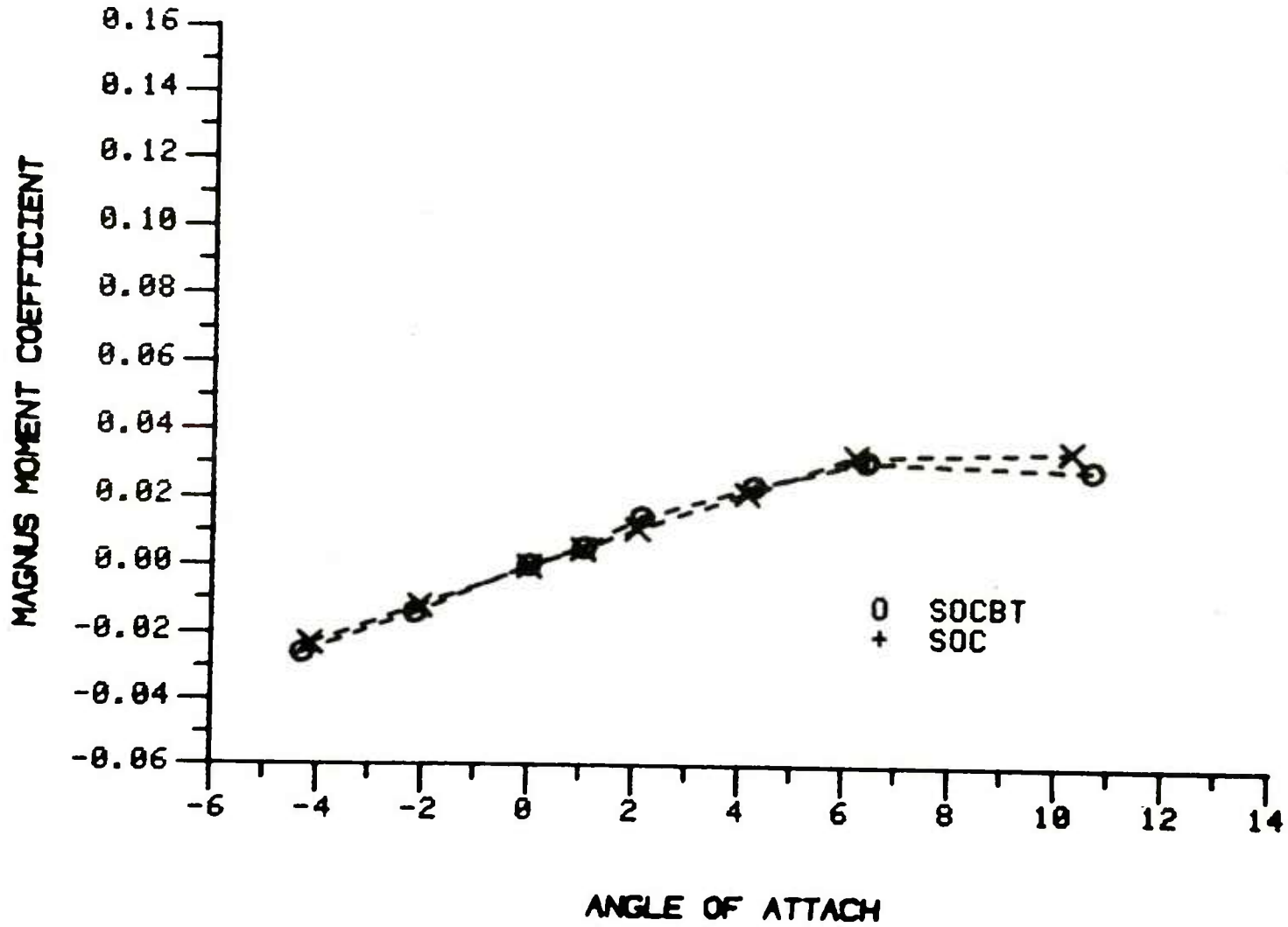

Figure 5. Boattail Effect on Magnus Moment Coefficient, M = 4.0

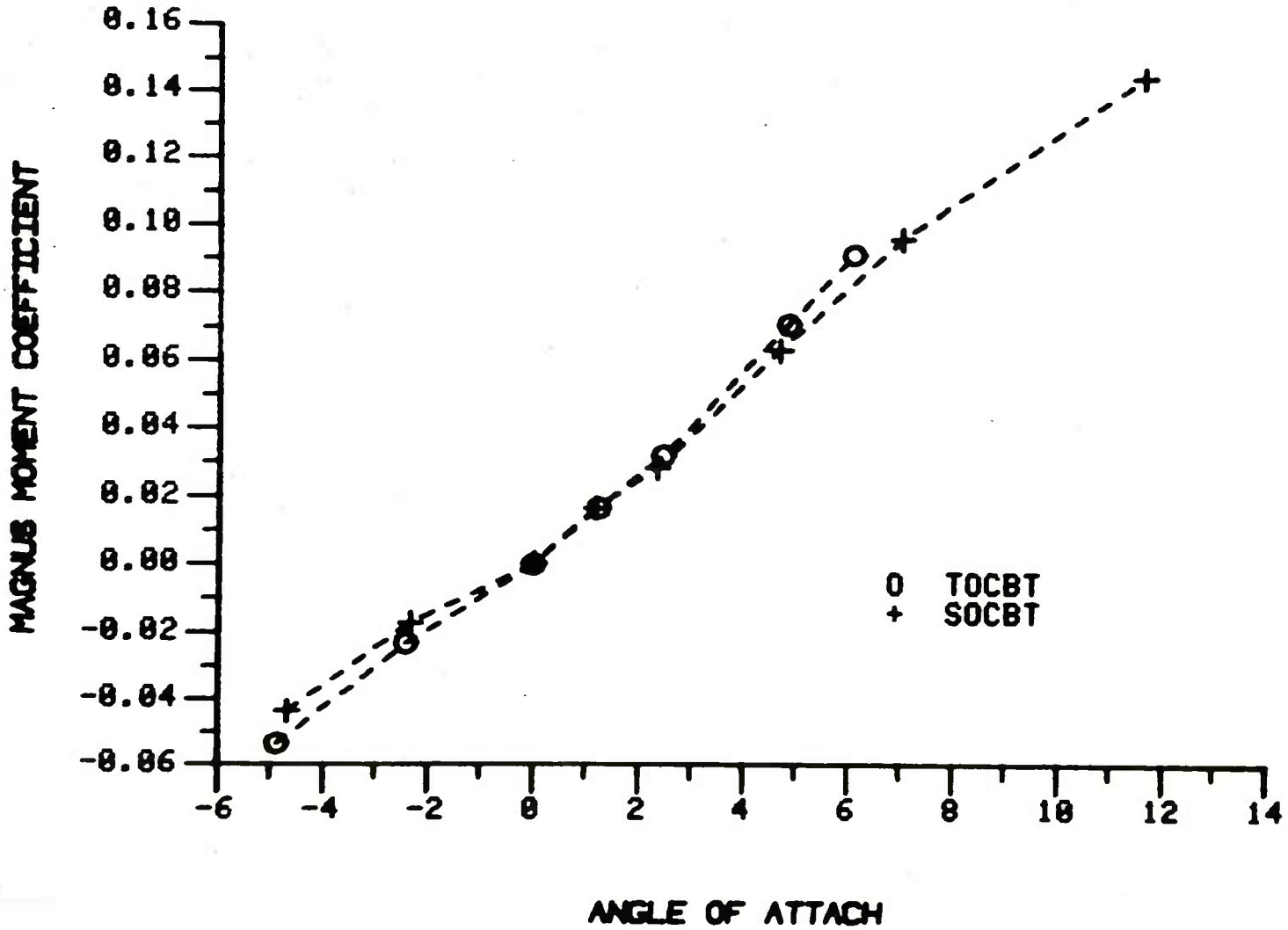

Figure 6. Ogive Effect on Magnus Moment Coefficient, M = 2.0

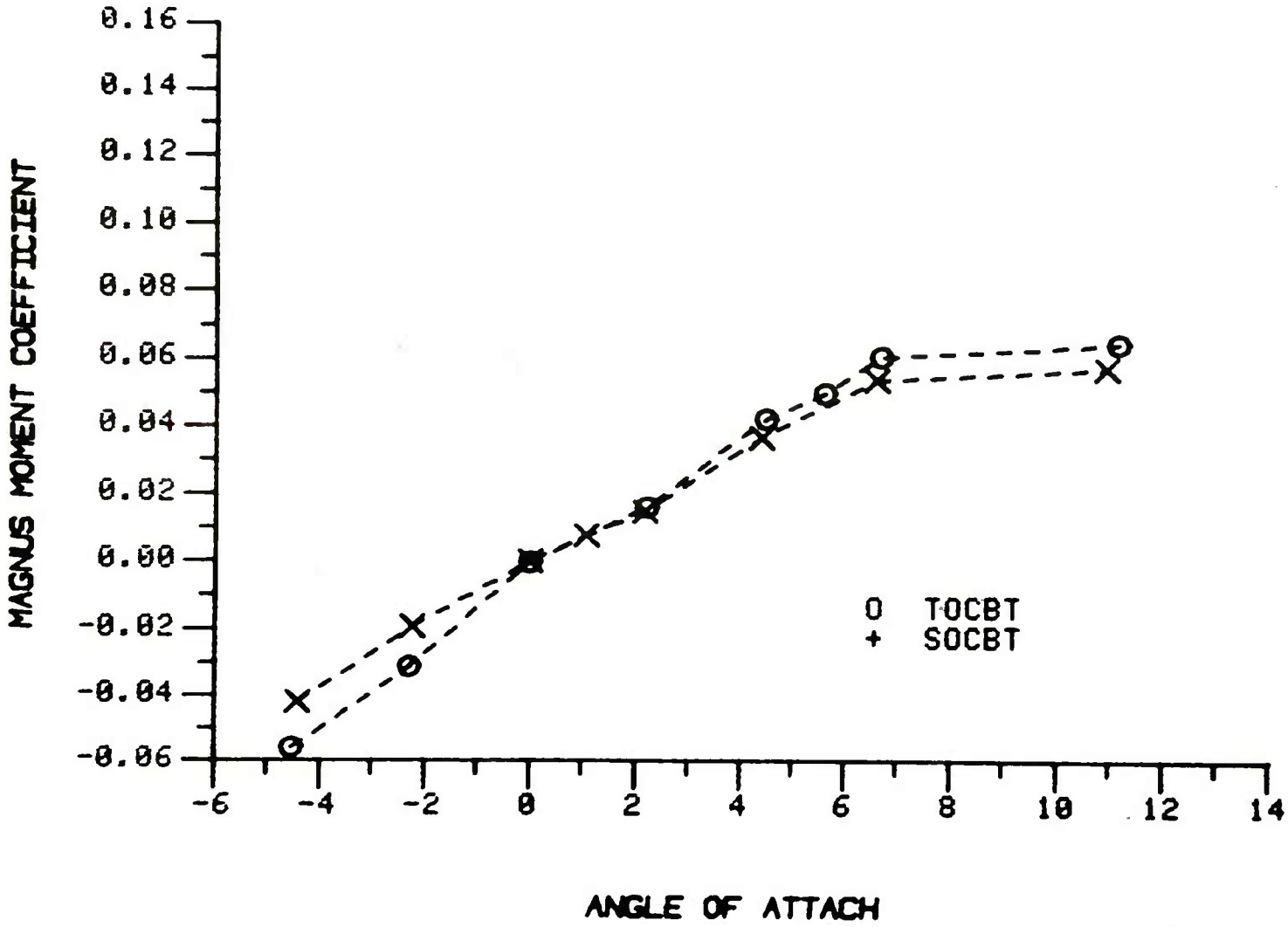

Figure 7. Ogive Effect on Magnus Moment Coefficient, M = 3.0

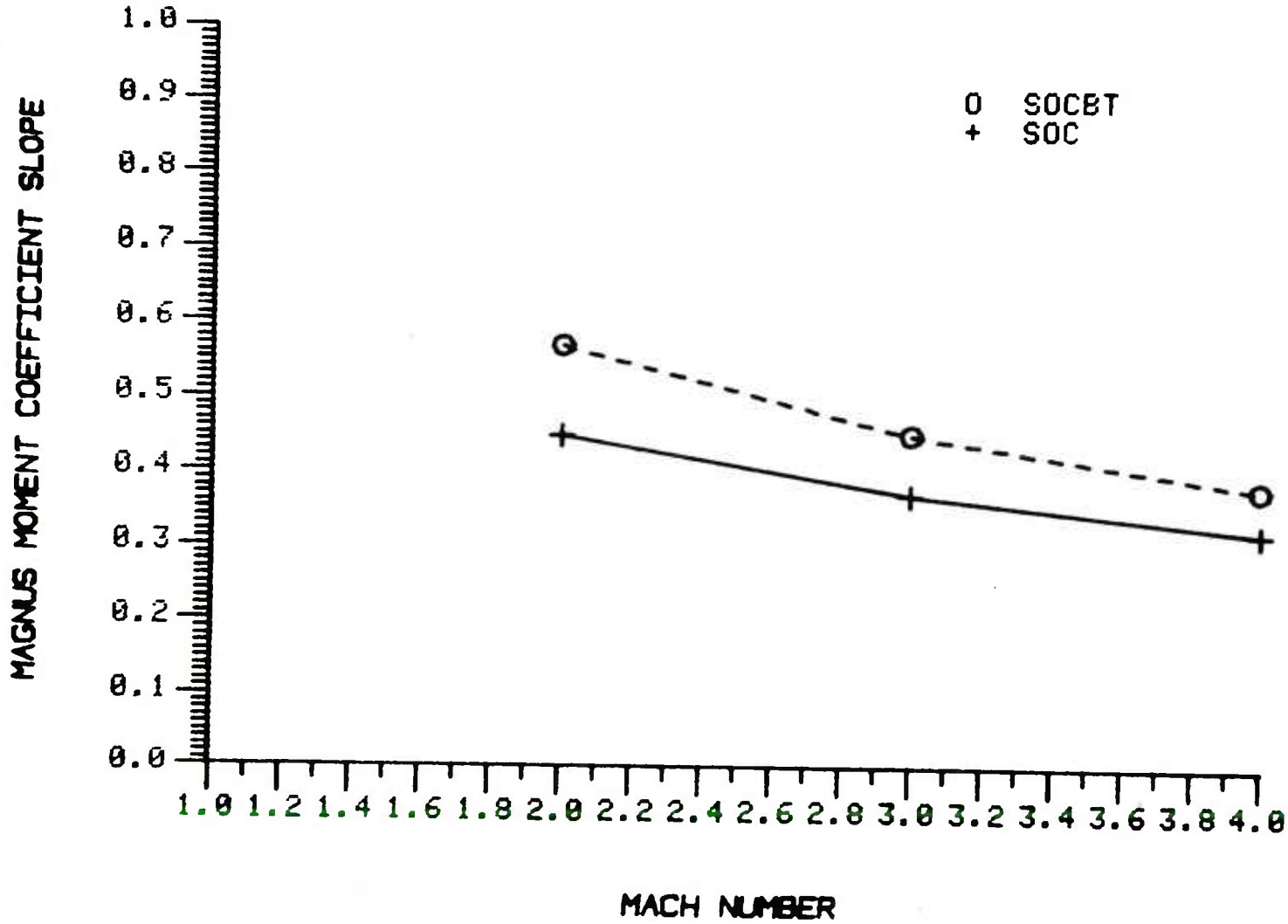

Figure 8. Magnus Moment Coefficient Slope vs Mach Number

Table III. Secant-Ogive-Cylinder and Secant-Ogive-Cylinder with Boattail Tabulated Pitch-Plane Force and Moment Data

TABULATED PITCH-PLANE FORCE AND MOMENT DATA

RUN NO.	MACH NO.	REYNOLDS NO*10E-6	P-ZERO MP	T-ZERO DEG K	NORMAL-FORCE COEFFS A1	A2	PITCHING MMT COEFFS B1	B2	CPN FR NOSE	AXL FC COEFFS CA	CAB	CONFIGURATION
32	2.00	8.6434	.2126	306.2	4.886-02	0.000	-1.135-01	0.000	2.3220	.2326	.1074	1 SOC
104	3.00	7.1878	.2976	309.7	5.396-02	0.000	-1.410-01	0.000	2.6130	.1791	.0691	1
123	4.00	7.3158	.5041	307.1	5.410-02	0.000	-1.453-01	0.000	2.6860	.1500	.0493	1
274	1.99	8.3827	.2130	316.4	4.394-02	0.000	-8.767-02	0.000	1.9950	.2214	.0531	3 SOCBT
204	2.99	7.2502	.2976	309.8	5.054-02	0.000	-1.199-01	0.000	2.3730	.1746	.0402	3
286	4.00	7.1585	.5009	309.5	5.032-02	0.000	-1.229-01	0.000	2.4420	.1527	.0331	3

LEGEND: REYNOLDS NUMBER = BASED ON MODEL LENGTH
P-ZERO = SUPPLY PRESSURE (MEGAPASCAL)
T-ZERO = SUPPLY TEMPERATURE (DEGREES KELVIN)

CN = A1*ALPHA+A2*ALPHA**2, NORMAL-FORCE COEFFICIENT
CM = B1*ALPHA+B2*ALPHA**2, PITCHING-MOMENT COEFFICIENT
CPN= NORMAL-FORCE, CENTER-OF-PRESSURE LOCATION,
DISTANCE FROM MODEL NOSE DIVIDED BY MODEL LENGTH
CA = TOTAL, AXIAL-FORCE COEFFICIENT AT ZERO ANGLE OF ATTACK
CAB= BASE-PRESSURE COEFFICIENT AT ZERO ANGLE OF ATTACK

MOMENTS ARE REFERENCED TO THE MODEL NOSE

Table IV. Secant-Ogive-Cylinder and Secant-Ogive-Cylinder with Boattail Tabulated Magnus Data

TABULATED MAGNUS AND BOUNDARY-LAYER TRANSITION DATA

RUN NO.	MACH NO.	REYNOLDS NO*10E-6	P-ZERO MP	T-ZERO DEG K	ALPHA DEGRS	MAGNUS FC COEFFS A1	MAGNUS FC COEFFS A2	MAGNUS MMT COEFFS B1	MAGNUS MMT COEFFS B2	CPY FR NOSE	B-L TRANSITION LEE	B-L TRANSITION WIND	CONFIGURATION
36	2.00	8.6591	.2128	306.2	10.81	-.113600	.000000	.565900	.000000	4.9600	.1184	.1184	1 SOC
37	2.00	8.6512	.2130	306.4	6.55	-.060260	.000000	.304400	.000000	5.0700	.1184	.1184	1
38	2.00	8.6480	.2128	306.5	4.38	-.035920	.000000	.177900	.000000	5.0400	.1184	.1184	1
39	2.00	8.6206	.2119	306.5	2.18	-.016450	.000000	.080230	.000000	4.9800	.1184	.1184	1
40	2.00	8.6342	.2127	306.8	1.08	-.009445	.000000	.048950	.000000	5.7500	.1184	.1184	1
43	2.00	8.6107	.2122	306.9	-.01	-.002992	.000000	.020570	.000000	6.6500	.1184	.1184	1
41	2.00	8.6284	.2125	306.9	-2.22	.015980	.000000	-.073620	.000000	4.5800	.1184	.1184	1
42	2.00	8.6234	.2128	306.9	-4.40	.034700	.000000	-.164500	.000000	4.6600	.1184	.1184	1
111	3.00	7.1419	.2972	310.9	10.40	-.068820	.000000	.327500	.000000	4.7400	.1184	.1184	1 SOC
112	3.00	7.1374	.2973	311.1	6.28	-.044000	.000000	.218600	.000000	5.0300	.1184	.1184	1
113	3.00	7.1320	.2972	311.1	4.20	-.026470	.000000	.129800	.000000	4.9800	.1184	.1184	1
116	3.00	7.1370	.2972	311.1	2.09	-.011470	.000000	.056770	.000000	4.8200	.1184	.1184	1
117	3.00	7.1520	.2975	311.2	1.03	-.005314	.000000	.026800	.000000	5.2800	.1184	.1184	1
120	3.00	7.1357	.2972	311.5	-.02	.000963	.000000	-.004437	.000000	4.1700	.1184	.1184	1
118	3.00	7.1435	.2971	311.4	-2.14	.014480	.000000	-.069600	.000000	4.7600	.1184	.1184	1
119	3.00	7.1371	.2967	311.3	-4.24	.029240	.000000	-.141700	.000000	4.8900	.1184	.1184	1
130	4.00	7.3234	.5046	306.6	10.28	-.037860	.000000	.178400	.000000	4.6700	.1184	.1184	1 SOC
131	4.00	7.3240	.5044	307.3	6.20	-.031080	.000000	.151300	.000000	4.8100	.1184	.1184	1
132	4.00	7.3177	.5045	307.4	4.14	-.020590	.000000	.101000	.000000	4.7800	.1184	.1184	1
134	4.00	7.3085	.5044	307.4	2.05	-.007972	.000000	.040960	.000000	5.0600	.1184	.1184	1
135	4.00	7.3018	.5047	307.0	1.01	-.002996	.000000	.016060	.000000	5.2300	.1184	.1184	1
138	4.00	7.2833	.5052	308.2	-.01	.001571	.000000	-.007247	.000000	4.0100	.1184	.1184	1
136	4.00	7.2954	.5038	307.3	-2.09	.012650	.000000	-.060710	.000000	4.7700	.1184	.1184	1
137	4.00	7.2890	.5044	307.5	-4.15	.023290	.000000	-.110700	.000000	4.8000	.1184	.1184	1

LEGEND: REYNOLDS NUMBER = BASED ON MODEL LENGTH
P-ZERO = SUPPLY PRESSURE (MEGAPASCAL)
T-ZERO = SUPPLY TEMPERATURE (DEGREES KELVIN)
ALPHA = ANGLE OF ATTACK (DEGREES)

CY = A1*(PD/V)+A2*(PD/V)**2, SIDE-FORCE COEFFICIENT
CYM = B1*(PD/V)+B2*(PD/V)**2, YAWING-MOMENT COEFFICIENT
CPY = MAGNUS-FORCE, CENTER-OF-PRESSURE LOCATION,
DISTANCE FROM MODEL NOSE DIVIDED BY MODEL LENGTH
B-L TRANSITION = DISTANCE FROM MODEL NOSE DIVIDED BY
MODEL LENGTH FOR LEE AND WIND SIDES OF THE MODEL;
EQUALS TRIP LOCATION FOR TRIPPED BOUNDARY-LAYER CONDITION
MOMENTS ARE REFERENCED TO THE MODEL NOSE

Table IV. (continued)

TABULATED MAGNUS AND BOUNDARY-LAYER TRANSITION DATA

RUN NO.	MACH NO.	REYNOLDS NO*10E-6	P-ZERO MP	T-ZERO DEG K	ALPHA DEGRS	MAGNUS FC COEFFS A1	MAGNUS FC COEFFS A2	MAGNUS MMT COEFFS B1	MAGNUS MMT COEFFS B2	CPY FR NOSE	B-L TRANSITION LEE	B-L TRANSITION WIND	CONFIGURATION
278	2.00	8.3475	.2128	314.3	11.65	-.134700	.000000	.654800	.000000	4.8500	.1184	.1184	3 SOCBT
279	2.00	8.3293	.2126	314.7	7.05	-.074730	.000000	.378800	.000000	5.0700	.1184	.1184	3
280	2.00	8.3179	.2126	315.1	4.68	-.045160	.000000	.230600	.000000	5.2100	.1184	.1184	3
281	2.00	8.3079	.2128	315.4	2.34	-.021790	.000000	.110900	.000000	5.0800	.1184	.1184	3
282	2.00	8.2994	.2128	315.6	1.18	-.014990	.000000	.069990	.000000	4.9400	.1184	.1184	3
285	2.00	8.2682	.2127	316.4	.01	-.000207	.000000	.000214	.000000	2.0900	.1184	.1184	3
283	2.00	8.2832	.2128	316.0	-2.35	.018480	.000000	-.088870	.000000	4.7200	.1184	.1184	3
284	2.00	8.2742	.2126	316.3	-4.69	.040740	.000000	-.199800	.000000	4.8400	.1184	.1184	3
206	3.00	7.1820	.2971	309.7	10.97	-.069790	.000000	.323200	.000000	4.5800	.1184	.1184	3 SOCBT
207	3.00	7.1866	.2970	309.5	6.60	-.047650	.000000	.233100	.000000	4.9000	.1184	.1184	3
208	3.00	7.1896	.2974	309.9	4.39	-.031040	.000000	.154900	.000000	4.9400	.1184	.1184	3
210	3.00	7.2013	.2976	309.4	2.18	-.013380	.000000	.068530	.000000	4.8100	.1184	.1184	3
211	3.00	7.2032	.2975	309.5	1.07	-.006850	.000000	.035730	.000000	4.7800	.1184	.1184	3
214	3.00	7.2104	.2977	309.3	-.02	.001085	.000000	-.005412	.000000	2.3100	.1184	.1184	3
212	3.00	7.2047	.2979	309.4	-2.23	.016890	.000000	-.082750	.000000	4.9500	.1184	.1184	3
213	3.00	7.2109	.2976	309.0	-4.43	.033260	.000000	-.163100	.000000	5.0900	.1184	.1184	3
288	4.00	7.1141	.5016	311.6	10.69	-.036690	.000000	.168100	.000000	4.5500	.1184	.1184	3 SOCBT
289	4.00	7.1005	.5016	312.0	6.42	-.032220	.000000	.155100	.000000	4.7100	.1184	.1184	3
293	4.00	7.2531	.5025	308.0	4.26	-.021290	.000000	.105500	.000000	4.8400	.1184	.1184	3
294	4.00	7.2313	.5030	308.7	2.13	-.010800	.000000	.054830	.000000	5.1100	.1184	.1184	3
295	4.00	7.2079	.5031	309.5	1.05	-.005721	.000000	.028540	.000000	4.5600	.1184	.1184	3
298	4.00	7.1554	.5028	311.0	-.01	.000280	.000000	-.000078	.000000	4.2900	.1184	.1184	3
296	4.00	7.1875	.5030	310.2	-2.16	.011470	.000000	-.056170	.000000	5.1100	.1184	.1184	3
297	4.00	7.1712	.5029	310.6	-4.29	.023160	.000000	-.111300	.000000	4.9600	.1184	.1184	3

LEGEND: REYNOLDS NUMBER = BASED ON MODEL LENGTH
P-ZERO = SUPPLY PRESSURE (MEGAPASCAL)
T-ZERO = SUPPLY TEMPERATURE (DEGREES KELVIN)
ALPHA = ANGLE OF ATTACK (DEGREES)

CY = A1*(PD/V)+A2*(PD/V)**2, SIDE-FORCE COEFFICIENT
CYM = B1*(PD/V)+B2*(PD/V)**2, YAWING-MOMENT COEFFICIENT
CPY = MAGNUS-FORCE, CENTER-OF-PRESSURE LOCATION,
DISTANCE FROM MODEL NOSE DIVIDED BY MODEL LENGTH
B-L TRANSITION = DISTANCE FROM MODEL NOSE DIVIDED BY
MODEL LENGTH FOR LEE AND WIND SIDES OF THE MODEL;
EQUALS TRIP LOCATION FOR TRIPPED BOUNDARY-LAYER CONDITION
MOMENTS ARE REFERENCED TO THE MODEL NOSE

Table V. Tangent-Ogive-Cylinder and Tangent-Ogive-Cylinder with Boattail
Tabulated Pitch-Plane Force and Moment Data

TABULATED PITCH-PLANE FORCE AND MOMENT DATA

RUN NO.	MACH NO.	REYNOLDS NO*10E-6	P-ZERO MP	T-ZERO DEG K	NORMAL-FORCE COEFFS A1	A2	PITCHING MMT COEFFS B1	B2	CPN FR NOSE	AXL FC COEFFS CA	CAB	CONFIGURATION
19	3.00	7.2427	.2973	308.5	5.673-02	0.000	-1.309-01	0.000	2.3070	.2291	.0966	5 TOC
53	2.00	8.6080	.2114	309.0	5.293-02	0.000	-9.910-02	0.000	1.9720	.2849	.1360	5 TOC
79	3.00	7.2751	.2961	309.9	5.331-02	0.000	-1.110-01	0.000	2.0830	.1988	.0398	7 TOCBT

LEGEND: REYNOLDS NUMBER = BASED ON MODEL LENGTH
P-ZERO = SUPPLY PRESSURE (MEGAPASCAL)
T-ZERO = SUPPLY TEMPERATURE (DEGREES KELVIN)

CN = A1*ALPHA+A2*ALPHA**2, NORMAL-FORCE COEFFICIENT
CM = B1*ALPHA+B2*ALPHA**2, PITCHING-MOMENT COEFFICIENT
CPN= NORMAL-FORCE, CENTER-OF-PRESSURE LOCATION,
DISTANCE FROM MODEL NOSE DIVIDED BY MODEL LENGTH
CA = TOTAL, AXIAL-FORCE COEFFICIENT AT ZERO ANGLE OF ATTACK
CAB= BASE-PRESSURE COEFFICIENT AT ZERO ANGLE OF ATTACK

MOMENTS ARE REFERENCED TO THE MODEL NOSE

Table VI. Tangent-Ogive-Cylinder and Tangent-Ogive-Cylinder with Boattail Tabulated Magnus Data

TABULATED MAGNUS AND BOUNDARY-LAYER TRANSITION DATA

RUN NO.	MACH NO.	REYNOLDS NO*10E-6	P-ZERO MP	T-ZERO DEG K	ALPHA DEGRS	MAGNUS FC COEFFS A1	MAGNUS FC COEFFS A2	MAGNUS MMT COEFFS B1	MAGNUS MMT COEFFS B2	CPY FR NOSE	B-L TRANSITION LEE	B-L TRANSITION WIND	CONFIGURATION
23	3.00	7.3035	.2970	306.1	11.11	-.084770	.000000	.395800	.000000	4.6500	.1184	.1184	5 TOC
25	3.00	7.2674	.2970	307.1	5.59	-.047140	.000000	.226000	.000000	4.8300	.1184	.1184	5
26	3.00	7.2648	.2968	307.1	4.45	-.035970	.000000	.173700	.000000	4.7500	.1184	.1184	5
27	3.00	7.2503	.2969	307.5	2.24	-.016520	.000000	.080600	.000000	4.8000	.1184	.1184	5
22	3.00	7.3332	.2971	305.3	.00	.001395	.000000	-.006928	.000000	4.9700	.1184	.1184	5
28	3.00	7.2364	.2985	307.9	-2.26	.021200	.000000	-.101300	.000000	5.2500	.1184	.1184	5
29	3.00	7.2372	.2969	308.0	-4.51	.040910	.000000	-.195200	.000000	4.8500	.1184	.1184	5
62	2.00	8.4555	.2108	309.4	11.85	-.157300	.000000	.750100	.000000	4.7600	.1184	.1184	5 TOC
61	2.00	8.4568	.2108	309.4	7.20	-.085740	.000000	.416800	.000000	4.9000	.1184	.1184	5
60	2.00	8.4510	.2108	309.5	6.04	-.066180	.000000	.318700	.000000	4.8500	.1184	.1184	5
58	2.00	8.4900	.2115	309.2	4.81	-.048250	.000000	.231100	.000000	4.8500	.1184	.1184	5
57	2.00	8.4936	.2115	309.1	2.41	-.021630	.000000	.103500	.000000	4.6000	.1184	.1184	5
54	2.00	8.4946	.2119	309.4	.00	.000246	.000000	-.000681	.000000	2.7600	.1184	.1184	5
56	2.00	8.4944	.2115	309.1	-2.40	.021250	.000000	-.099490	.000000	4.7000	.1184	.1184	5
55	2.00	8.4943	.2113	309.0	-4.82	.046190	.000000	-.216200	.000000	4.7300	.1184	.1184	5
82	3.00	7.1849	.2969	309.6	11.18	-.082070	.000000	.376800	.000000	4.5500	.1184	.1184	7 TOCBT
83	3.00	7.1833	.2970	309.6	6.70	-.058920	.000000	.282600	.000000	4.8000	.1184	.1184	7
84	3.00	7.1848	.2970	309.5	5.62	-.049400	.000000	.237500	.000000	4.7700	.1184	.1184	7
87	3.00	7.1796	.2967	309.5	4.48	-.036660	.000000	.181600	.000000	4.9100	.1184	.1184	7
88	3.00	7.1767	.2968	309.6	2.22	-.016760	.000000	.082400	.000000	4.6600	.1184	.1184	7
85	3.00	7.1898	.2970	309.5	.00	.001395	.000000	-.004000	.000000	4.9400	.1184	.1184	7
89	3.00	7.1835	.2968	309.5	-2.30	.021610	.000000	-.106900	.000000	5.3500	.1184	.1184	7
90	3.00	7.1840	.2967	309.5	-4.53	.040560	.000000	-.198800	.000000	5.2700	.1184	.1184	7

LEGEND: REYNOLDS NUMBER = BASED ON MODEL LENGTH
P-ZERO = SUPPLY PRESSURE (MEGAPASCAL)
T-ZERO = SUPPLY TEMPERATURE (DEGREES KELVIN)
ALPHA = ANGLE OF ATTACK (DEGREES)

CY = A1*(PD/V)+A2*(PD/V)**2, SIDE-FORCE COEFFICIENT
CYM = B1*(PD/V)+B2*(PD/V)**2, YAWING-MOMENT COEFFICIENT
CPY = MAGNUS-FORCE, CENTER-OF-PRESSURE LOCATION,
DISTANCE FROM MODEL NOSE DIVIDED BY MODEL LENGTH
B-L TRANSITION = DISTANCE FROM MODEL NOSE DIVIDED BY
MODEL LENGTH FOR LEE AND WIND SIDES OF THE MODEL;
EQUALS TRIP LOCATION FOR TRIPPED BOUNDARY-LAYER CONDITION
MOMENTS ARE REFERENCED TO THE MODEL NOSE

Table VI. (continued)

TABULATED MAGNUS AND BOUNDARY-LAYER TRANSITION DATA

RUN NO.	MACH NO.	REYNOLDS NO*10E-6	P-ZERO MP	T-ZERO DEG K	ALPHA DEGRS	MAGNUS FC COEFFS A1	MAGNUS FC COEFFS A2	MAGNUS MMT COEFFS B1	MAGNUS MMT COEFFS B2	CPY FR NOSE	B-L TRANSITION LEE	B-L TRANSITION WIND	CONFIGURATIO
124	2.00	8.5095	.2114	308.5	6.11	-.073600	.000000	.367200	.000000	5.0300	.1184	.1184	7 TOC
126	2.00	8.5077	.2117	309.0	4.87	-.055580	.000000	.277400	.000000	5.0800	.1184	.1184	7
127	2.00	8.5117	.2117	308.9	2.44	-.025790	.000000	.129600	.000000	5.0200	.1184	.1184	7
128	2.00	8.5212	.2117	308.6	1.23	-.013900	.000000	.070260	.000000	4.9300	.1184	.1184	7
123	2.00	8.5141	.2117	308.9	.00	.000724	.000000	-.002401	.000000	3.3160	.1184	.1184	7
129	2.00	8.5248	.2115	308.4	-2.42	.022170	.000000	-.105800	.000000	4.8500	.1184	.1184	7
130	2.00	8.5250	.2115	308.3	-4.87	.051700	.000000	-.250400	.000000	4.8100	.1184	.1184	7

LEGEND: REYNOLDS NUMBER = BASED ON MODEL LENGTH
P-ZERO = SUPPLY PRESSURE (MEGAPASCAL)
T-ZERO = SUPPLY TEMPERATURE (DEGREES KELVIN)
ALPHA = ANGLE OF ATTACK (DEGREES)

CY = A1*(PD/V)+A2*(PD/V)**2, SIDE-FORCE COEFFICIENT
CYM = B1*(PD/V)+B2*(PD/V)**2, YAWING-MOMENT COEFFICIENT
CPY = MAGNUS-FORCE, CENTER-OF-PRESSURE LOCATION,
DISTANCE FROM MODEL NOSE DIVIDED BY MODEL LENGTH
B-L TRANSITION = DISTANCE FROM MODEL NOSE DIVIDED BY
MODEL LENGTH FOR LEE AND WIND SIDES OF THE MODEL;
EQUALS TRIP LOCATION FOR TRIPPED BOUNDARY-LAYER CONDITION
MOMENTS ARE REFERENCED TO THE MODEL NOSE

LIST OF SYMBOLS

C_A	axial-force coefficient, $F_A/(qS)$
C_{Ab}	base-axial-force coefficient, $(p - p_b)\ S_b/(qS)$
C_n	yawing moment coefficient, yawing moment/qSd, reference at the nose of model
C_M	pitching-moment coefficient, pitching moment/(qSd), reference at the nose of the model
C_{M_p}	Magnus-moment coefficient, $\partial C_n/\partial(Pd/V)$
$C_{M_{p_\alpha}}$	slope of the Magnus-moment coefficient, $\partial C_{M_p}/\partial\alpha$
C_{M_α}	slope of the pitching-moment curve, $\partial C_M/\partial\alpha$, for $-1.5 \leqslant \alpha \leqslant 1.5$
C_N	normal-force coefficient, $F_N/(qS)$
C_{N_α}	slope of the normal-force curve, $\partial C_N/\partial\alpha$, for $-1.5 \leqslant \alpha \leqslant 1.5$
C_Y	side-force coefficient, $F_Y/(qS)$
d	reference diameter, 57.15 mm
d_b	diameter of the model base
F_A	axial force
F_N	normal force
F_Y	side force
M_∞	Mach number
p	free-stream static pressure
P	spin rate (Rad/Sec)
p_b	base pressure

LIST OF SYMBOLS (Continued)

Pd/V	non-dimensional spin rate
q	free-stream dynamic pressure
Re_{ℓ}	Reynolds number, based on free-stream conditions and total model length
S	reference area, $\pi d^2/4$
S_b	area of the model base, $\pi d_b^2/4$
V	free-stream velocity
α	angle of attack

APPENDIX A

Magnus and Pitch Data

for

SOC

SOCBT

Secant-Ogive-Cylinder and Secant-Ogive-Cylinder with Boattail

SOC AND SOCBT (Continued)

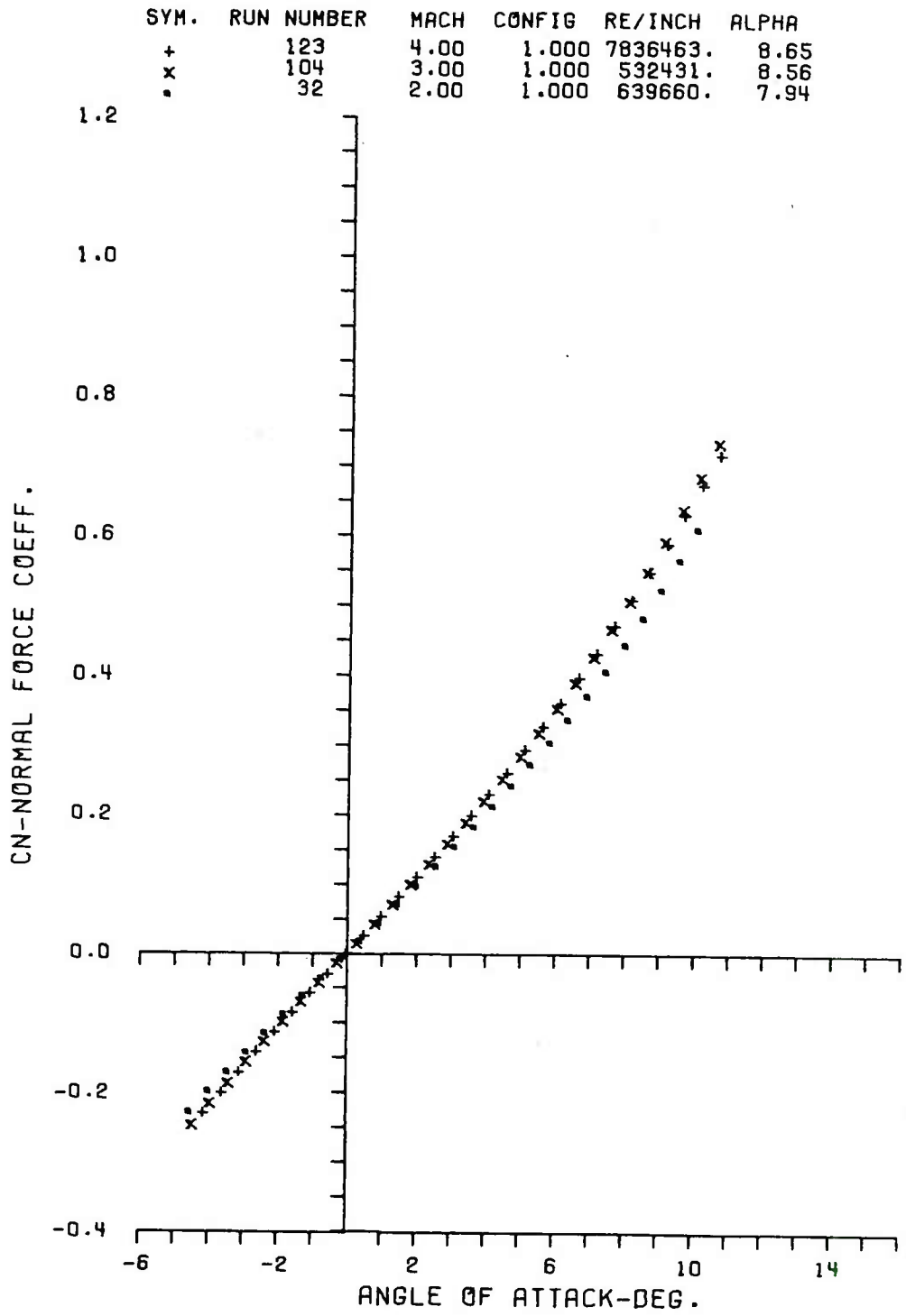

Figure A1. Normal Force Coefficient, C_N, Versus Angle of Attack

a. Secant-Ogive-Cylinder

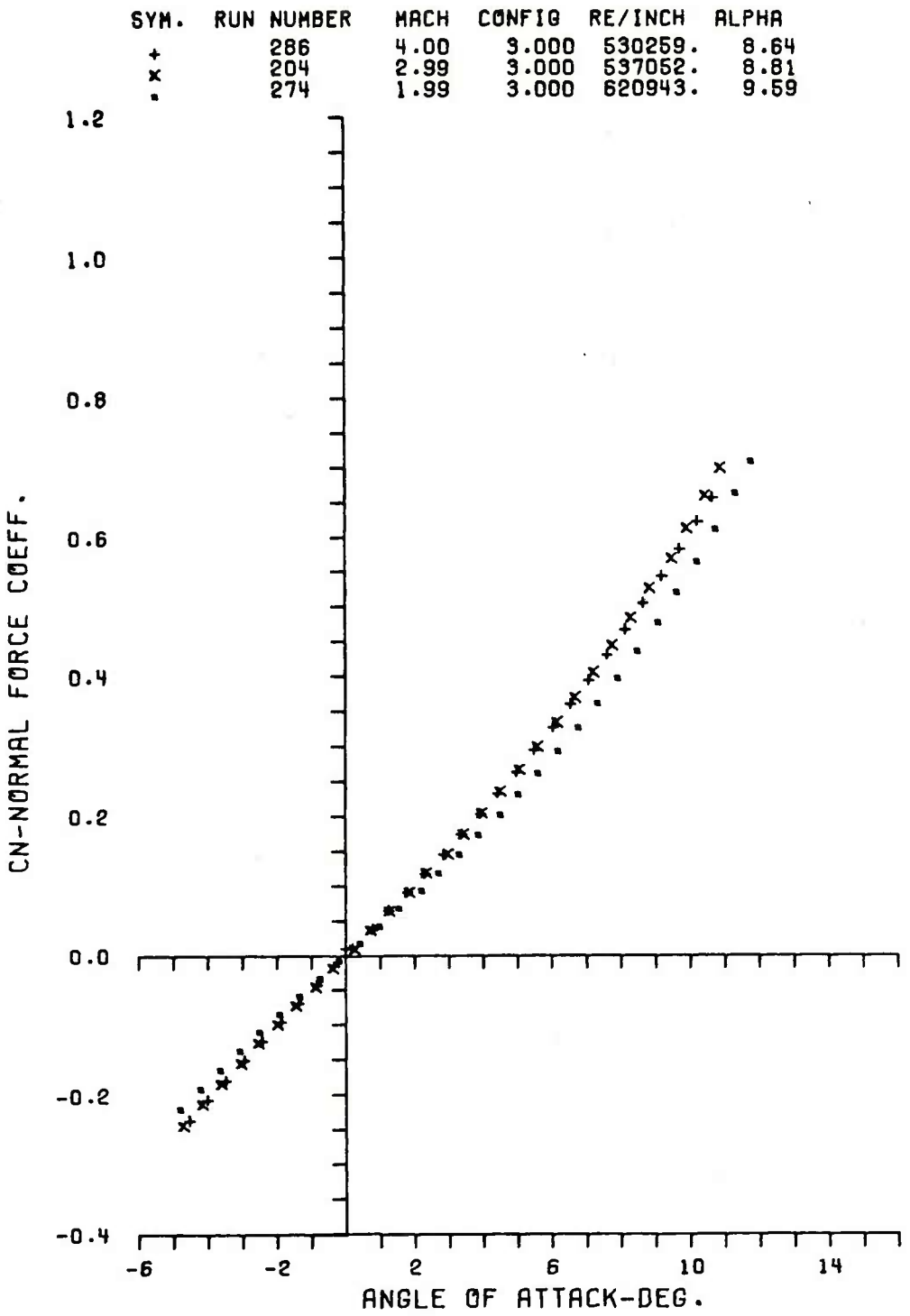

Figure A1. Continued

b. Secant-Ogive-Cylinder with Boattail

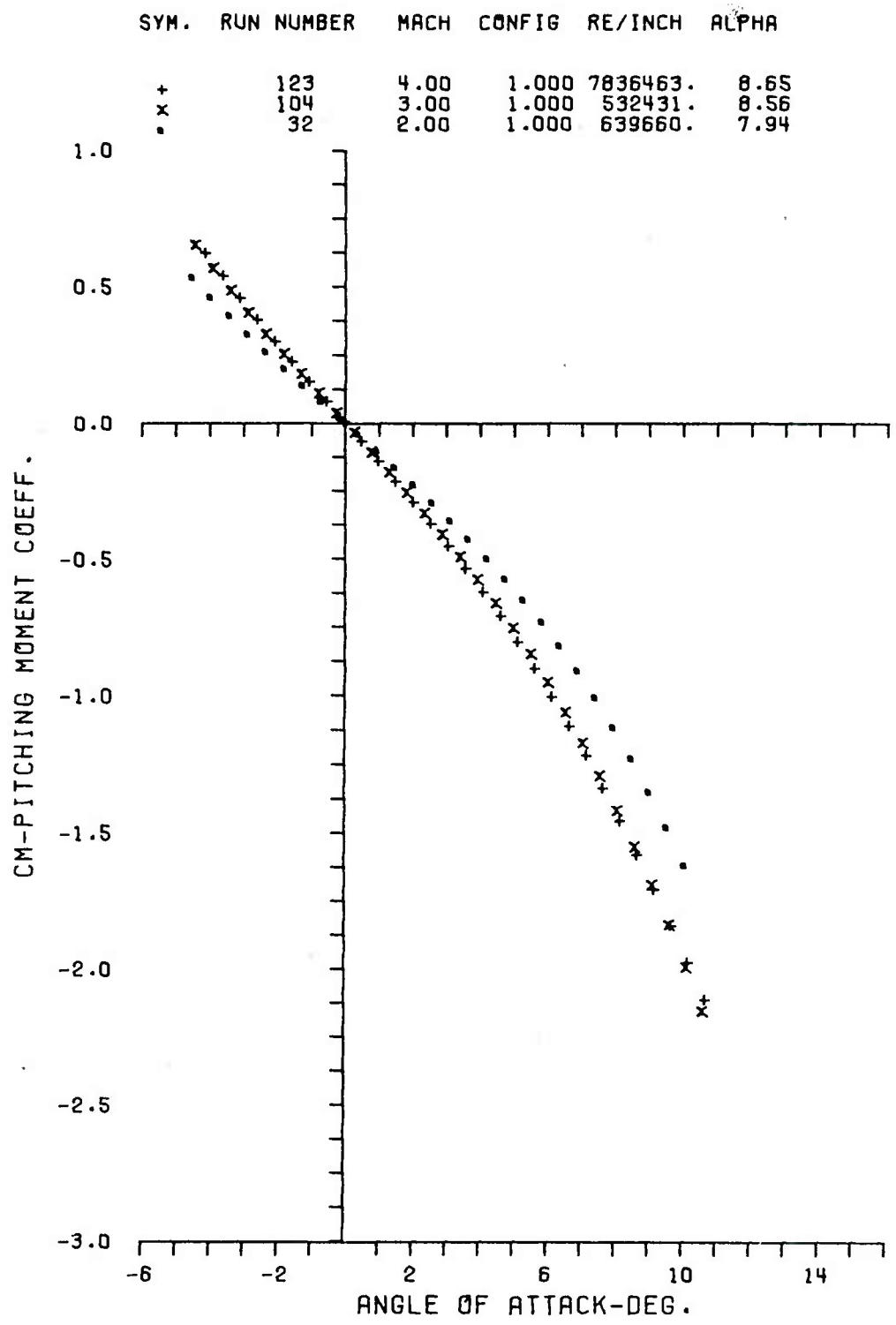

Figure A2. Pitching Moment Coefficient, C_M, Versus Angle of Attack

a. Secant-Ogive-Cylinder

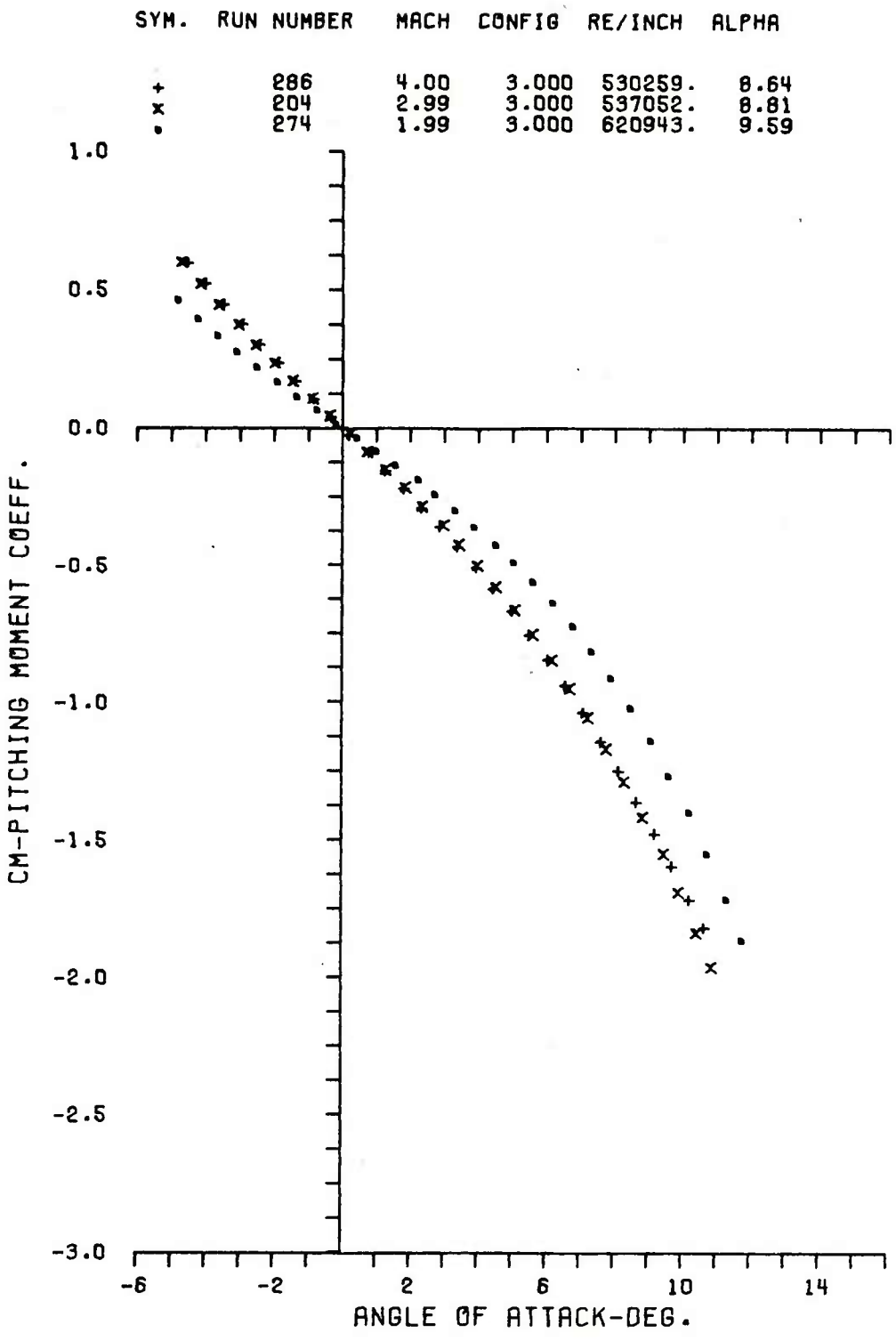

Figure A2. Continued

b. Secant-Ogive-Cylinder with Boattail

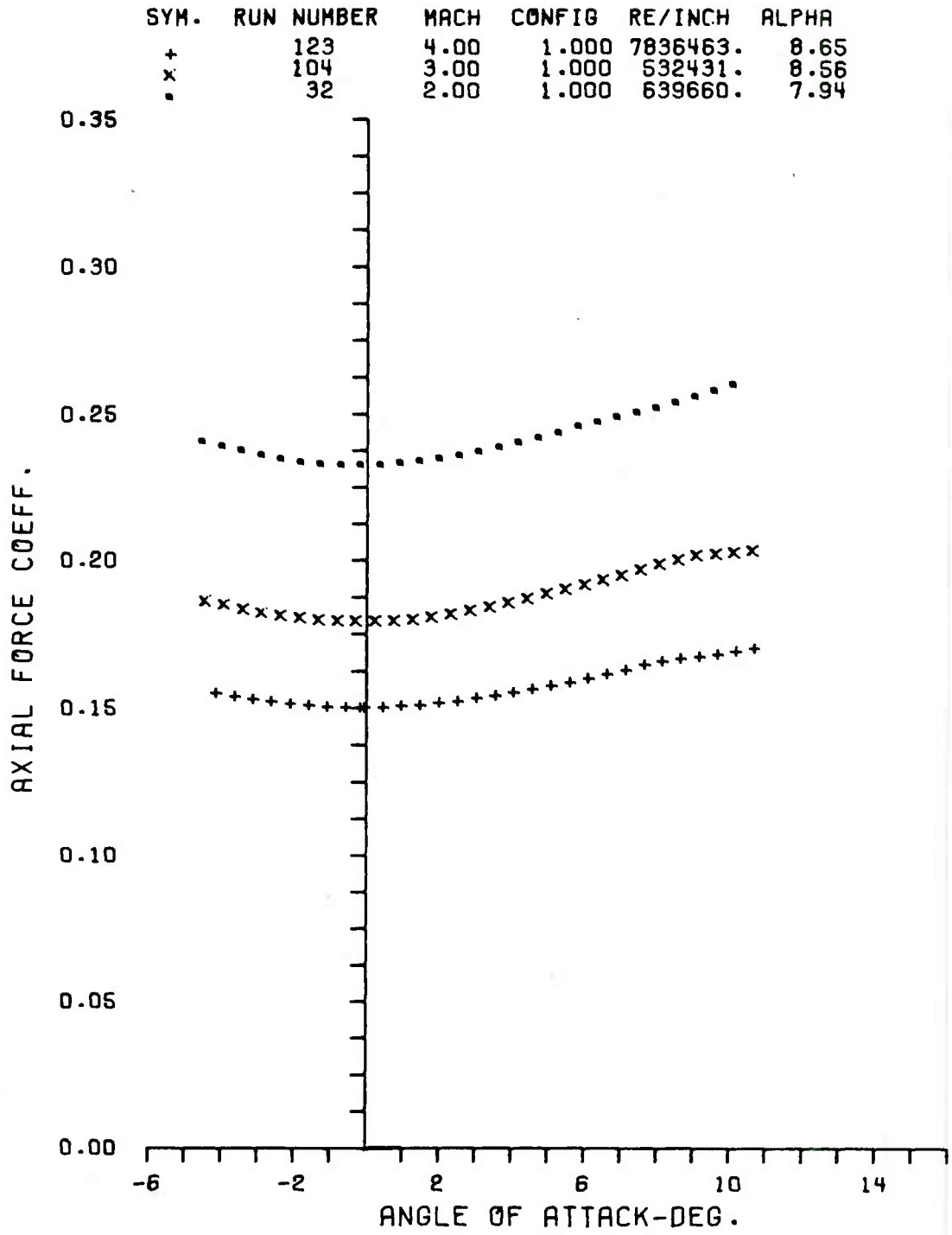

Figure A3. Axial Force Coefficient, C_A, Versus Angle of Attack

a. Secant-Ogive-Cylinder

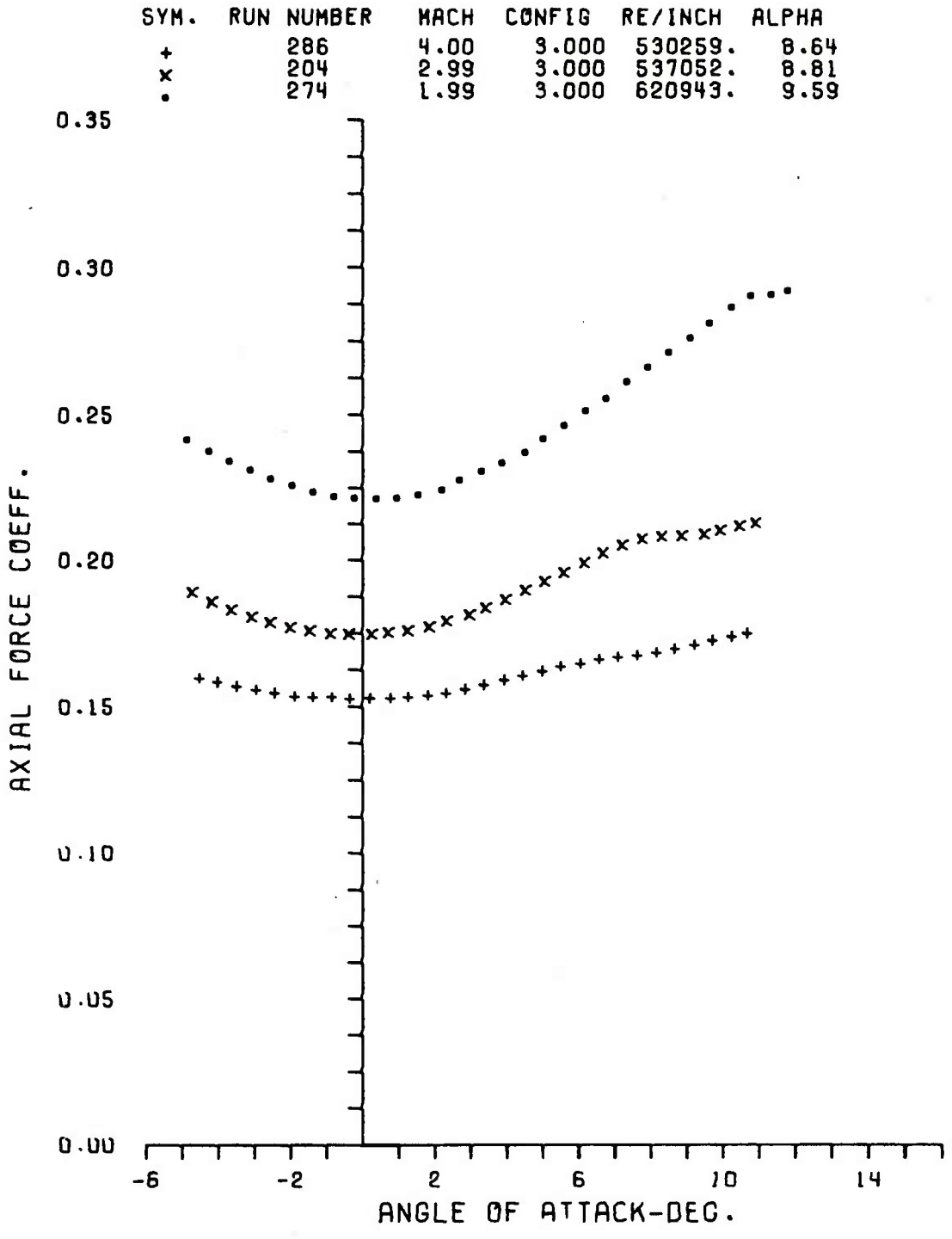

Figure A3. Continued

b. Secant-Ogive-Cylinder with Boattail

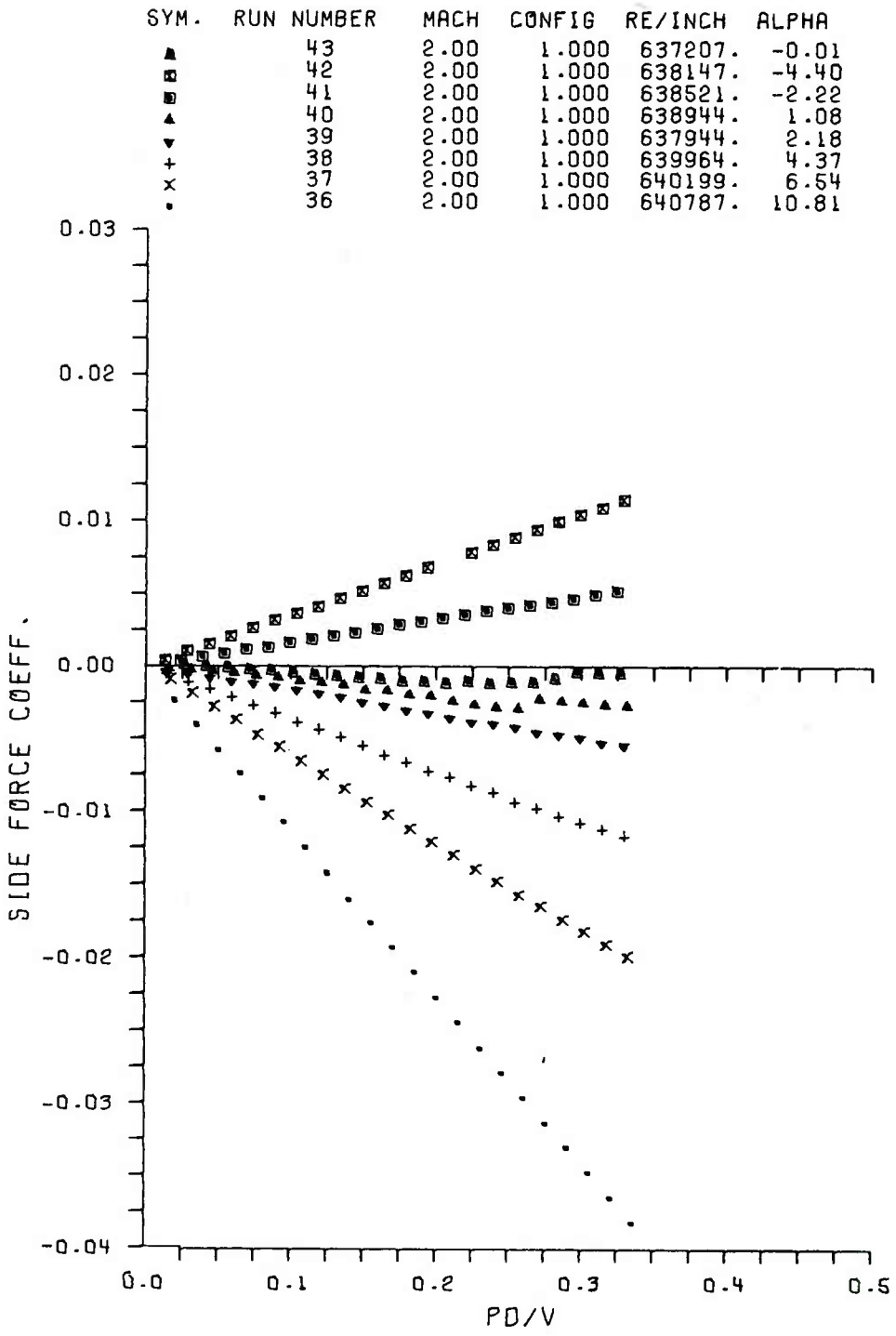

Figure A4. Side Force Coefficient, C_Y, Versus Spin Rate, Pd/V - Secant-Ogive-Cylinder

a. M = 2.0

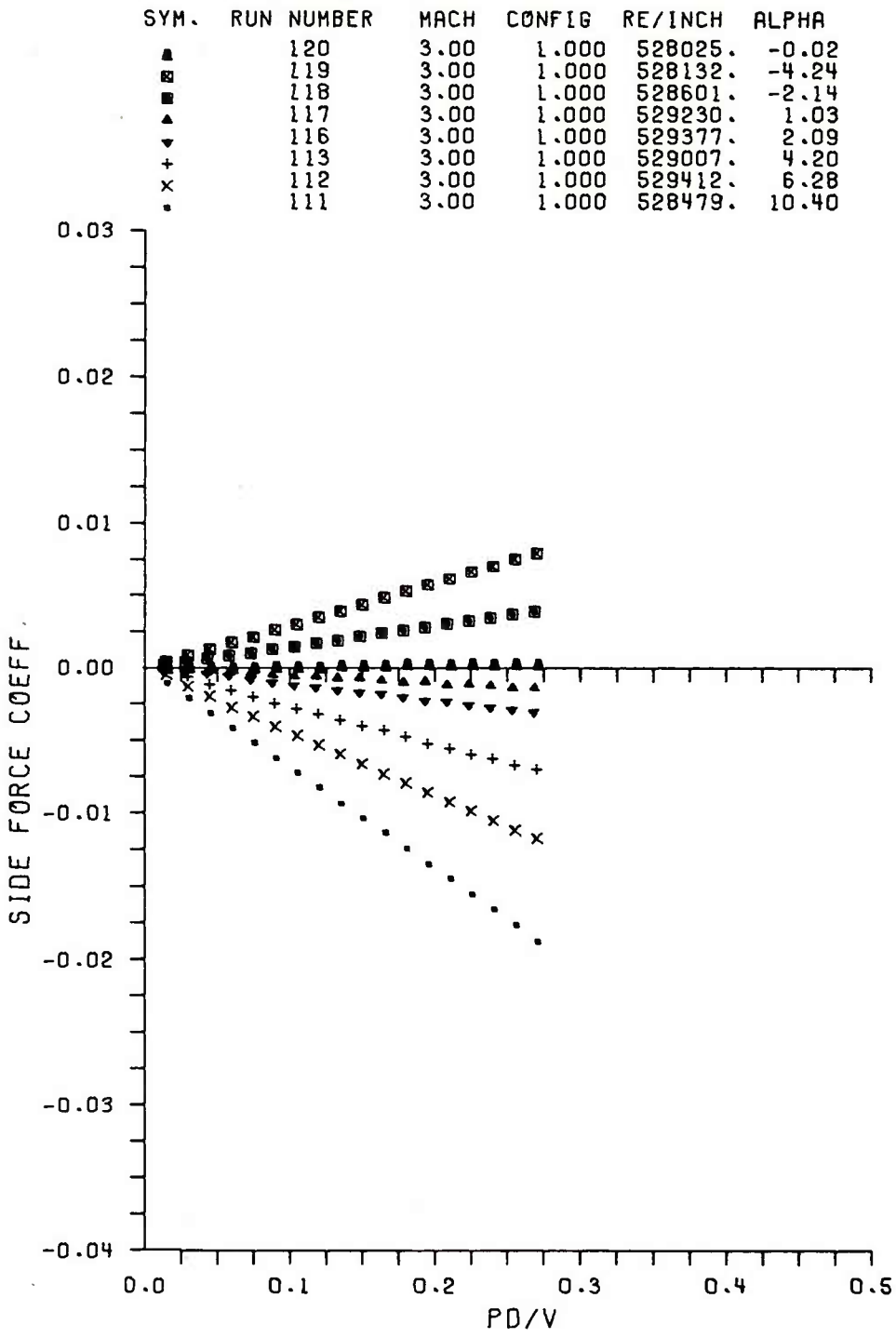

Figure A4. Continued

b. M = 3.0

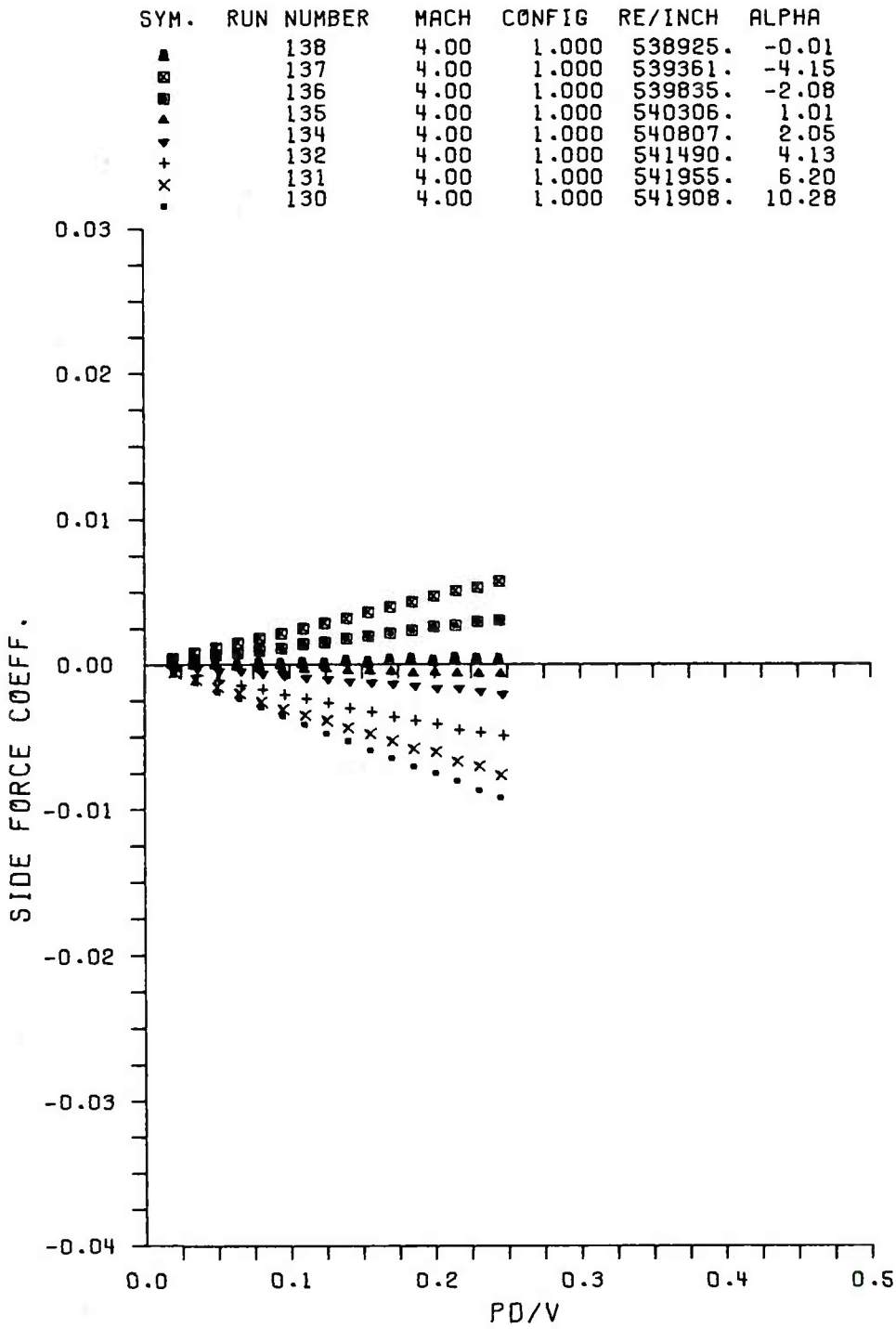

Figure A4. Continued

c. M = 4.0

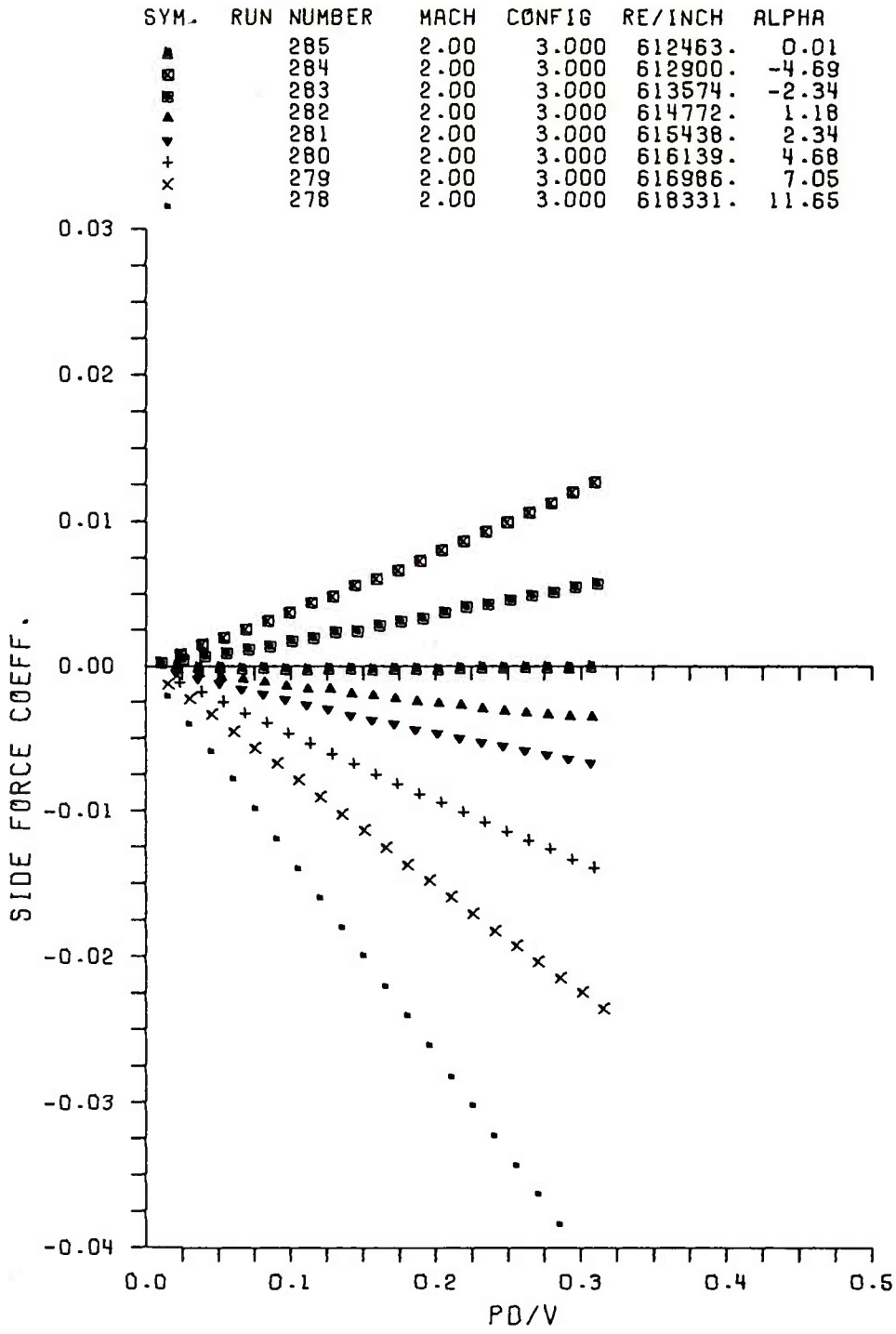

Figure A5. Side Force Coefficient, C_Y, Versus Spin Rate, Pd/V - Secant-Ogive-Cylinder with Boattail

a. M = 2.0

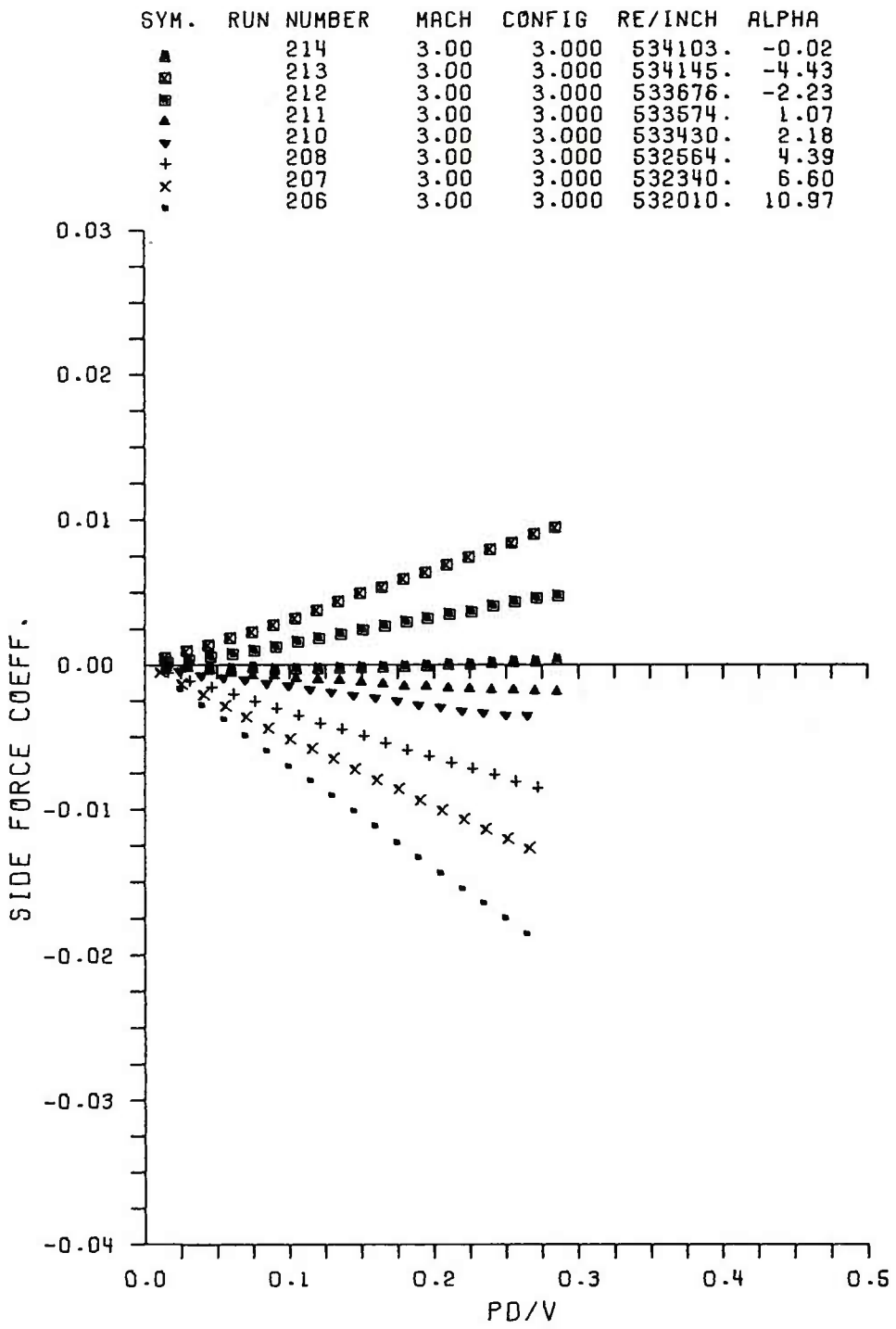

Figure A5. Continued

b. M = 3.0

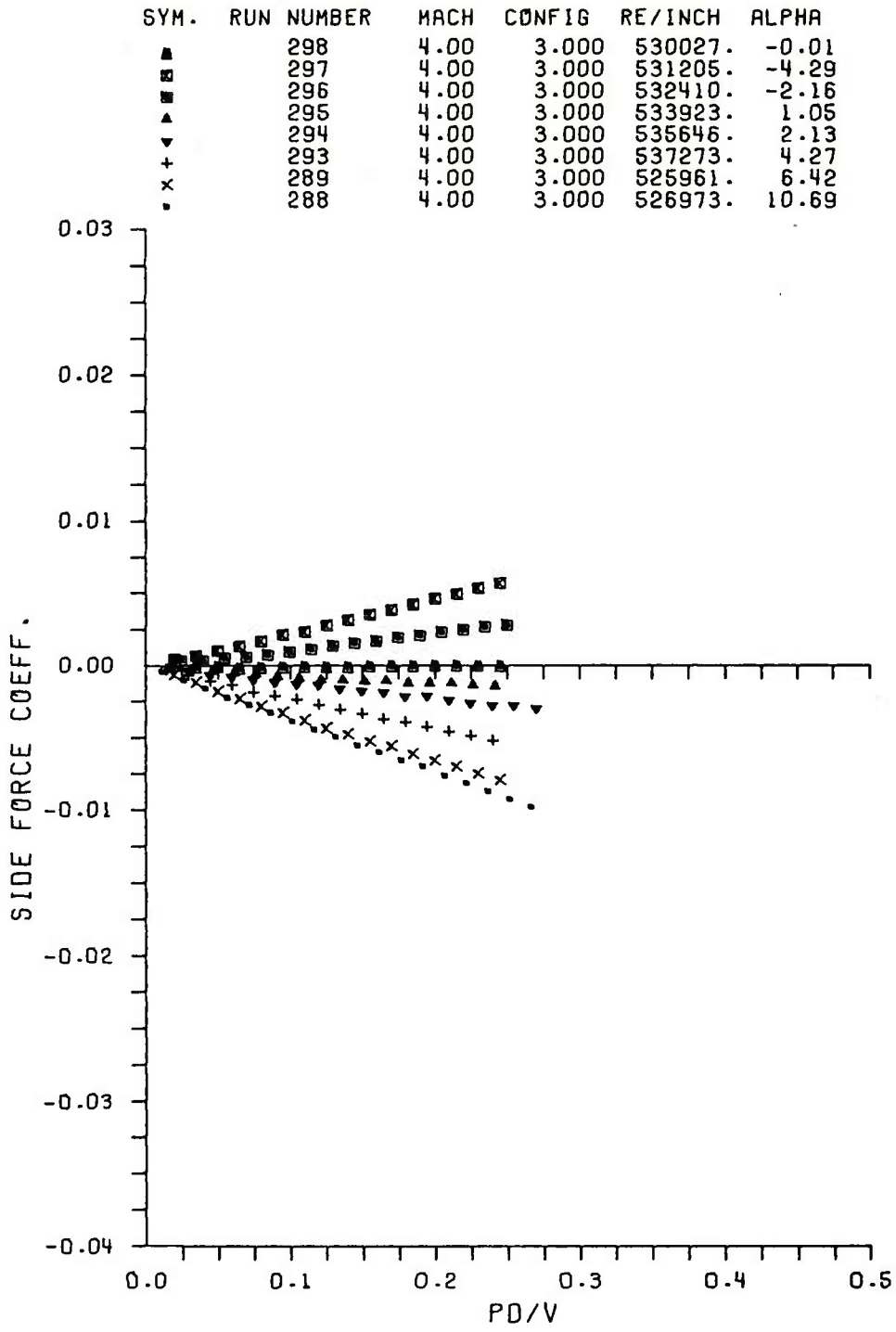

Figure A5. Continued

c. M = 4.0

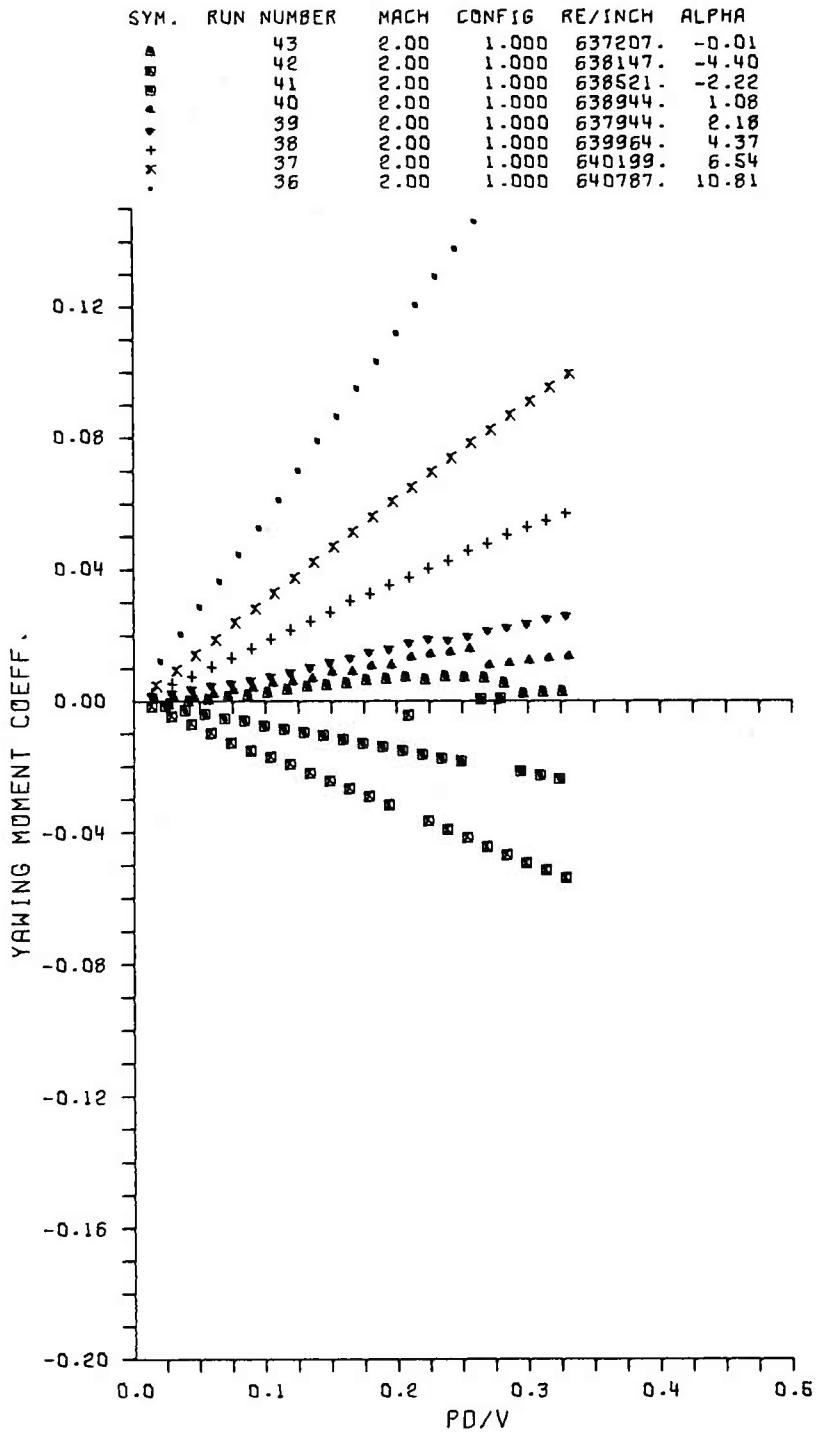

Figure A6. Yawing Moment Coefficient, C_n, Versus Spin Rate, Pd/V - Secant-Ogive-Cylinder

a. M = 2.0

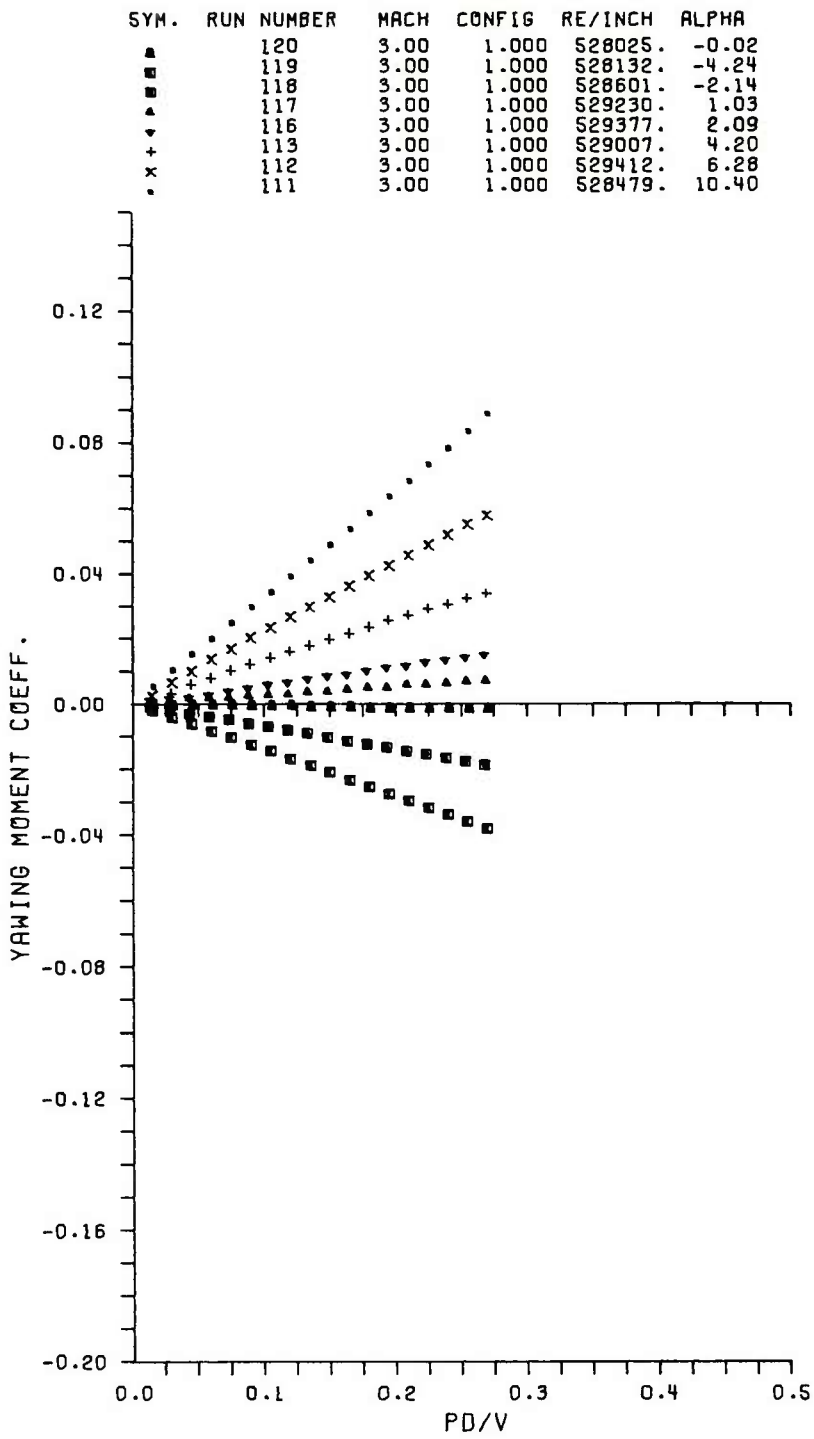

Figure A6. Continued

b. M = 3.0

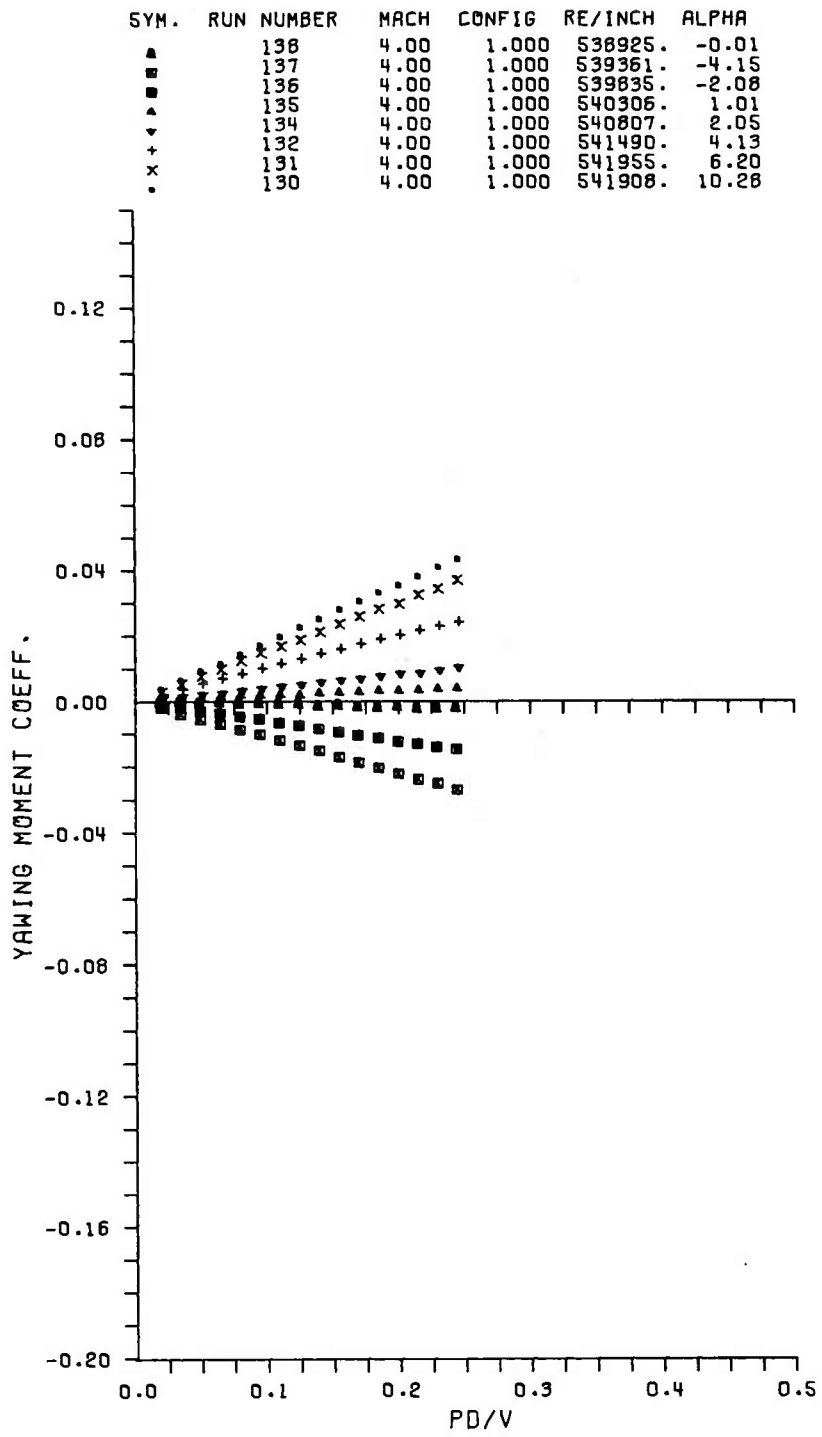

Figure A6. Continued

c. M = 4.0

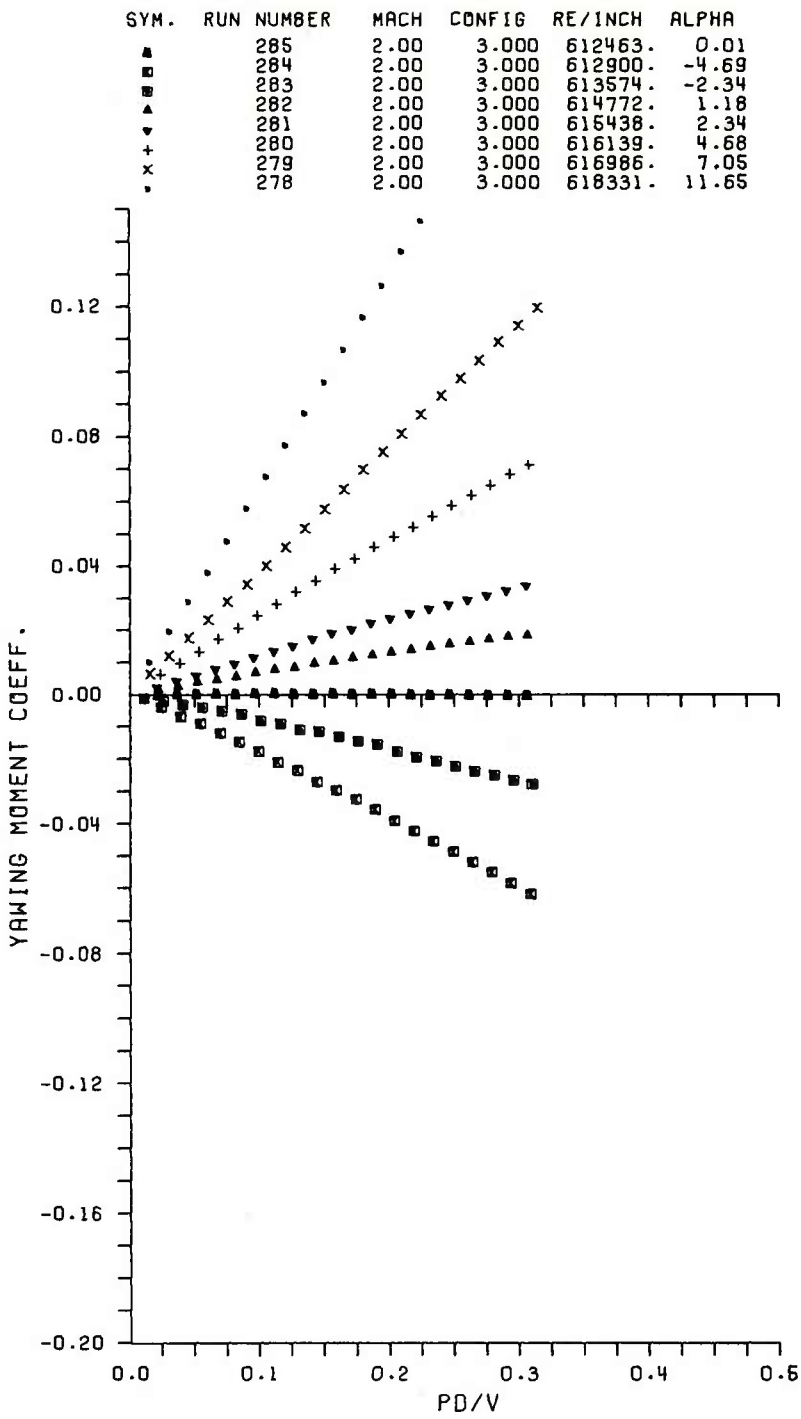

Figure A7. Yawing Moment Coefficient, C_n, Versus Spin Rate, Pd/V - Secant-Ogive-Cylinder with Boattail

a. M = 2.0

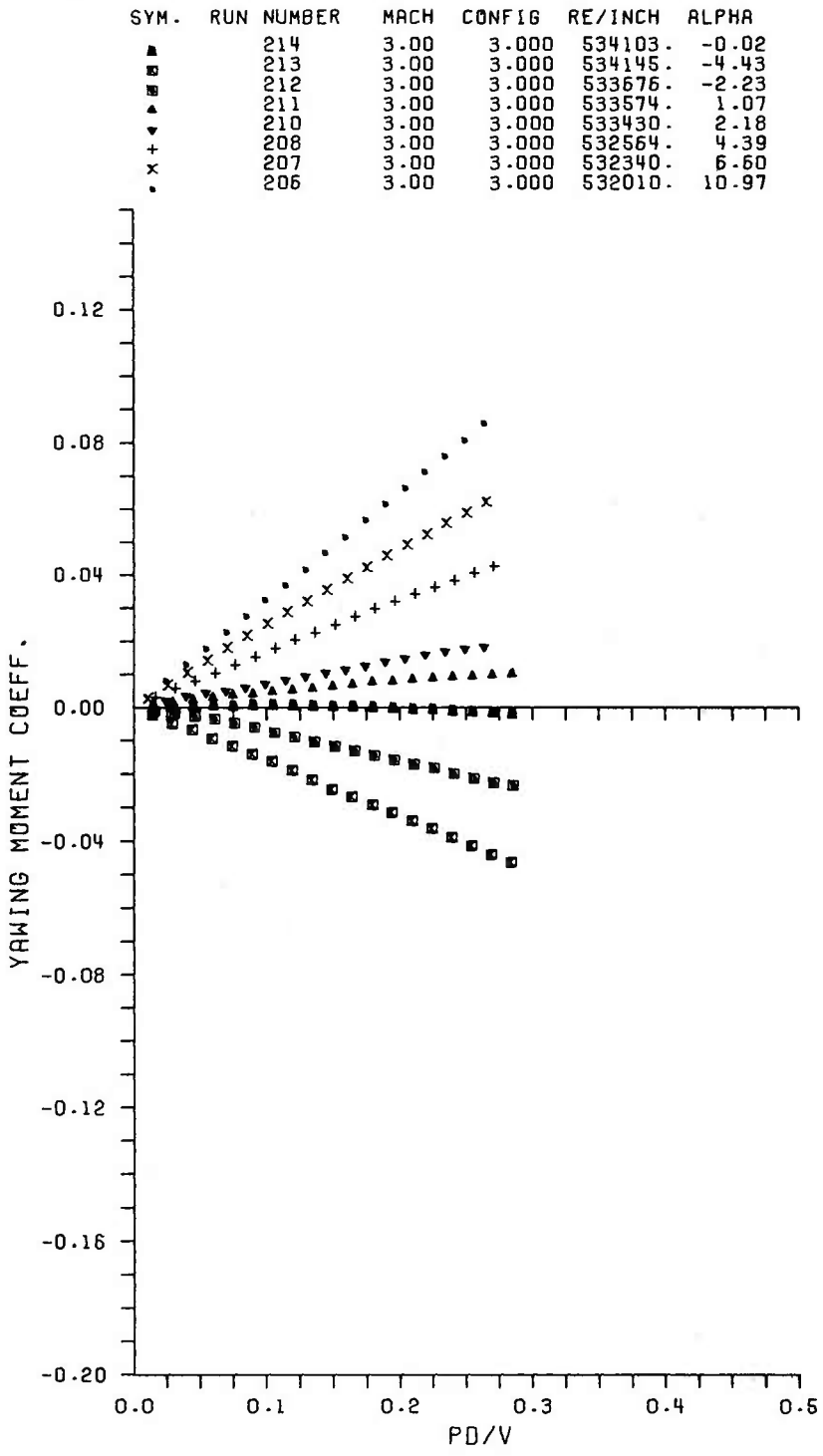

Figure A7. Continued

b. M = 3.0

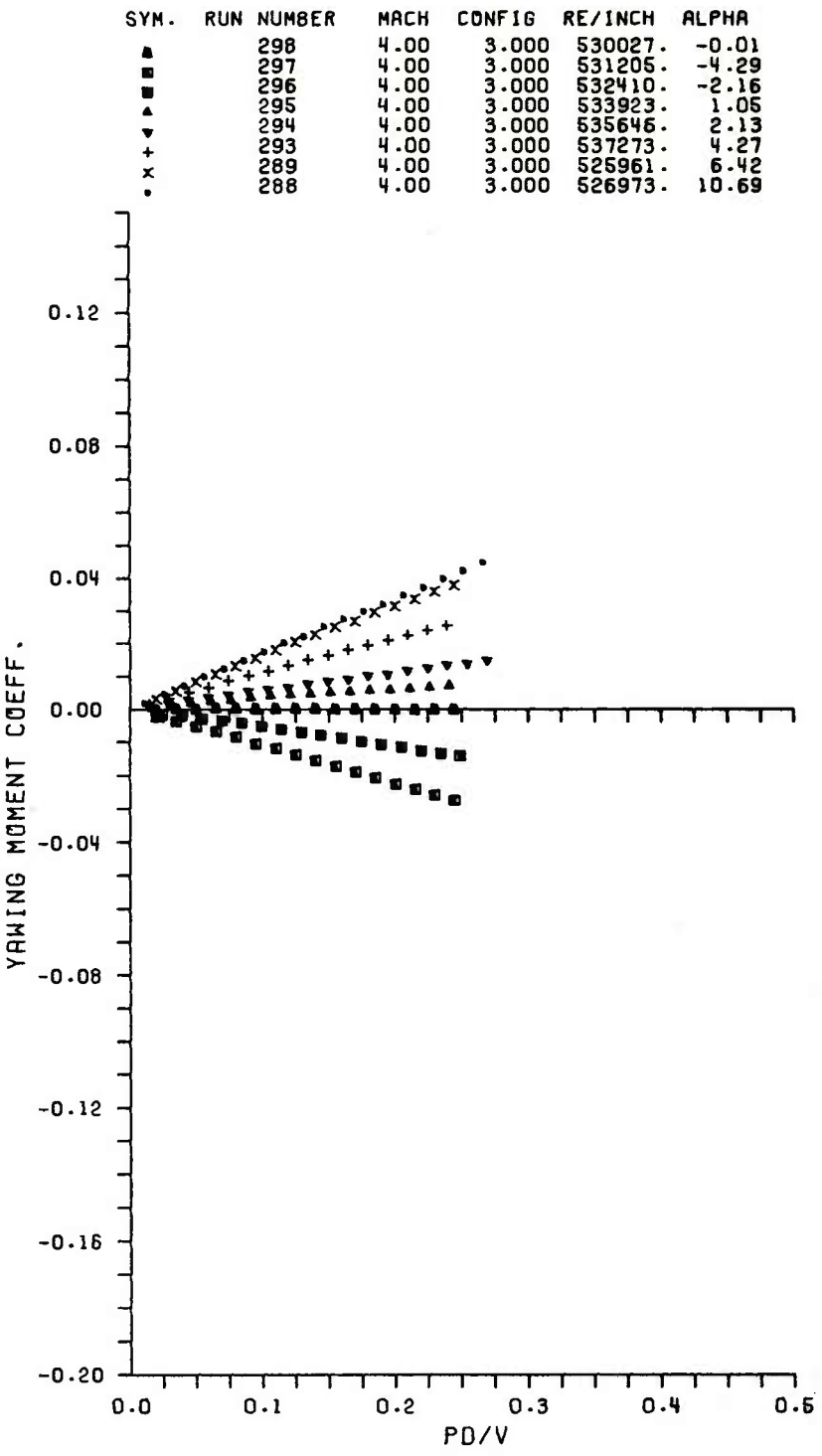

Figure A7. Continued

c. M = 4.0

APPENDIX B

Magnus and Pitch Data

for

TOC

TOCBT

Tangent-Ogive-Cylinder and Tangent-Ogive-Cylinder with Boattail

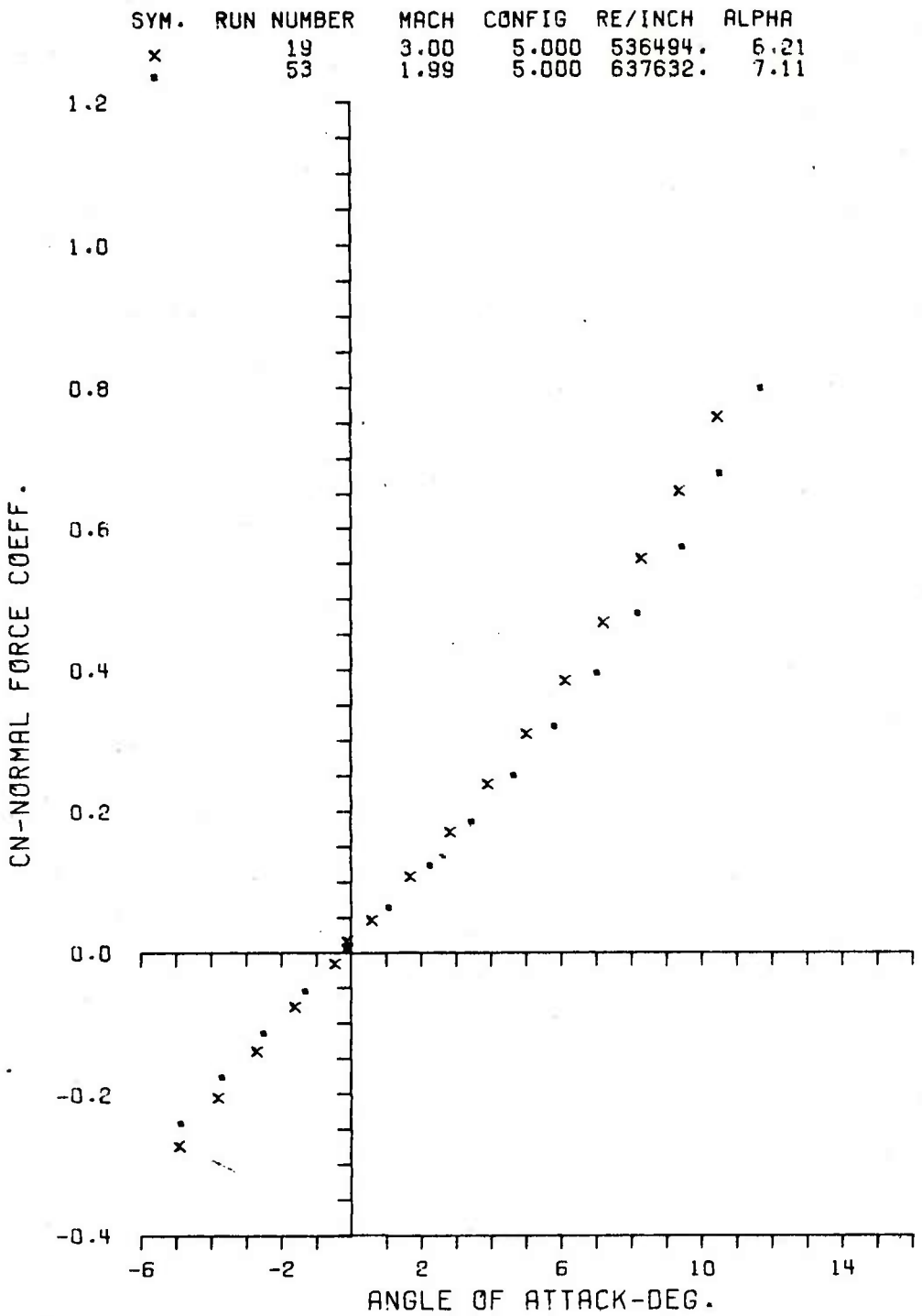

Figure B1. Normal Force Coefficient, C_N, Versus Angle of Attack

a. Tangent-Ogive-Cylinder

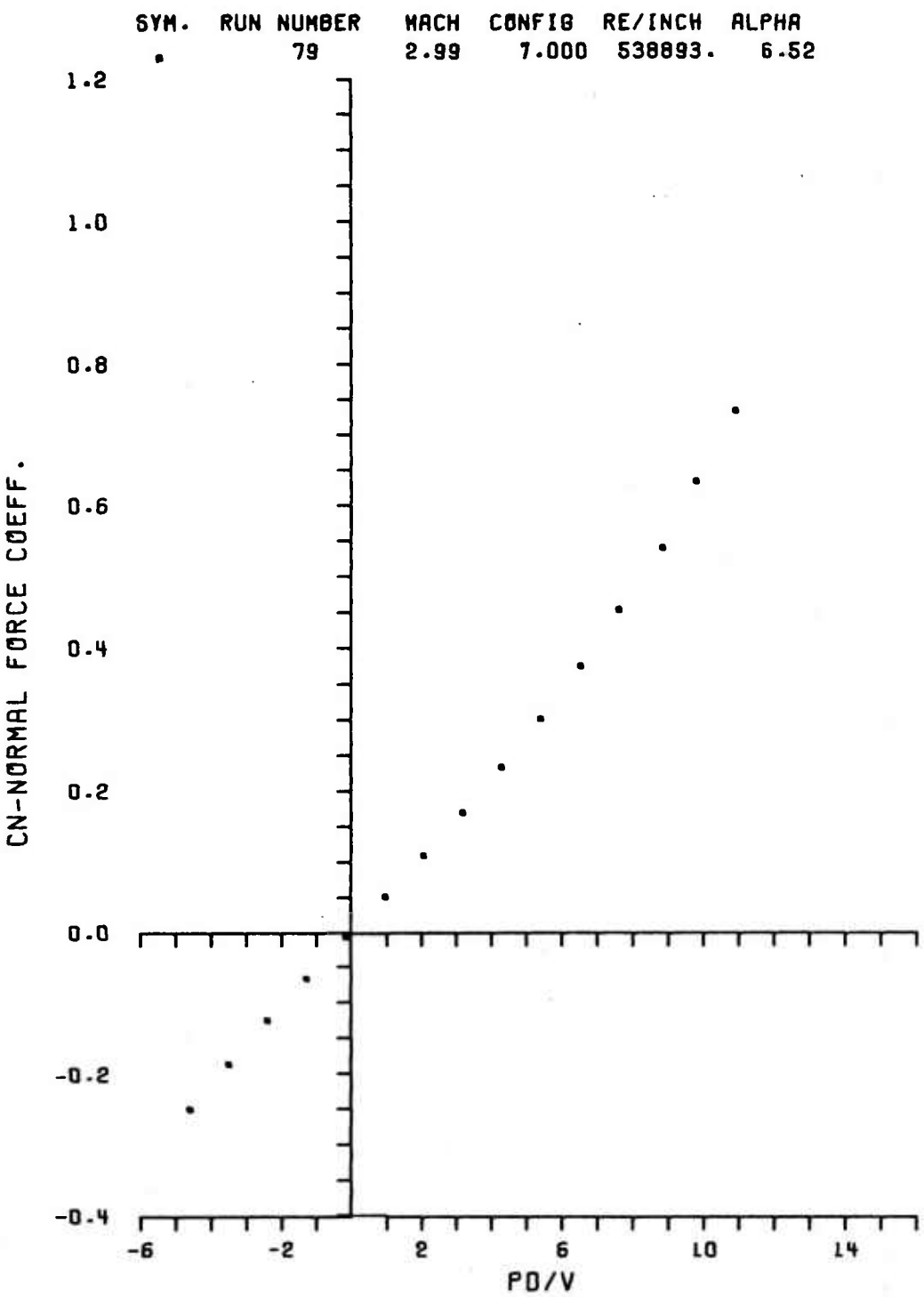

Figure B1. Continued

b. Tangent-Ogive-Cylinder with Boattail

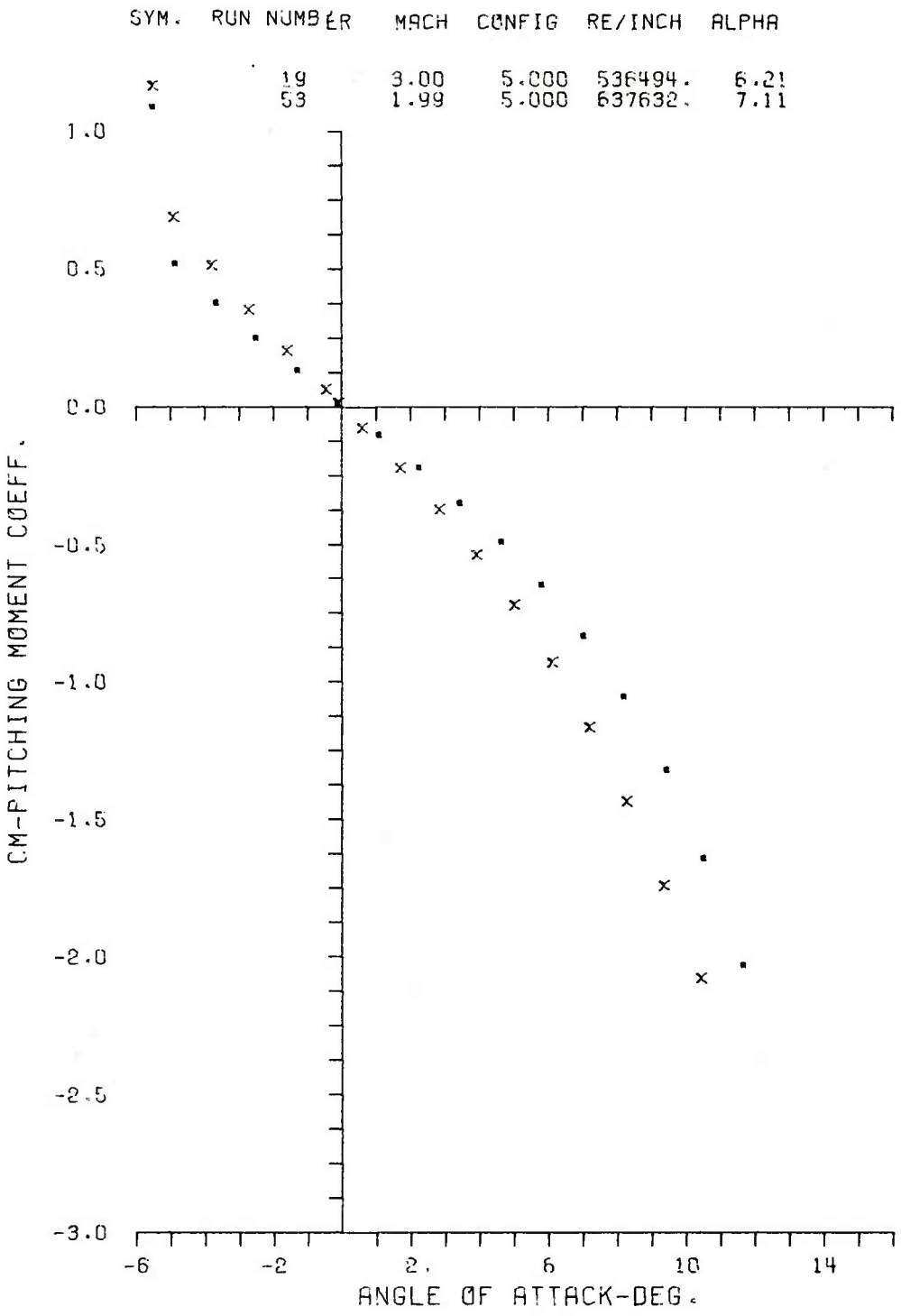

Figure B2. Pitching Moment Coefficient, C_M, Versus Angle of Attack

a. Tangent-Ogive-Cylinder

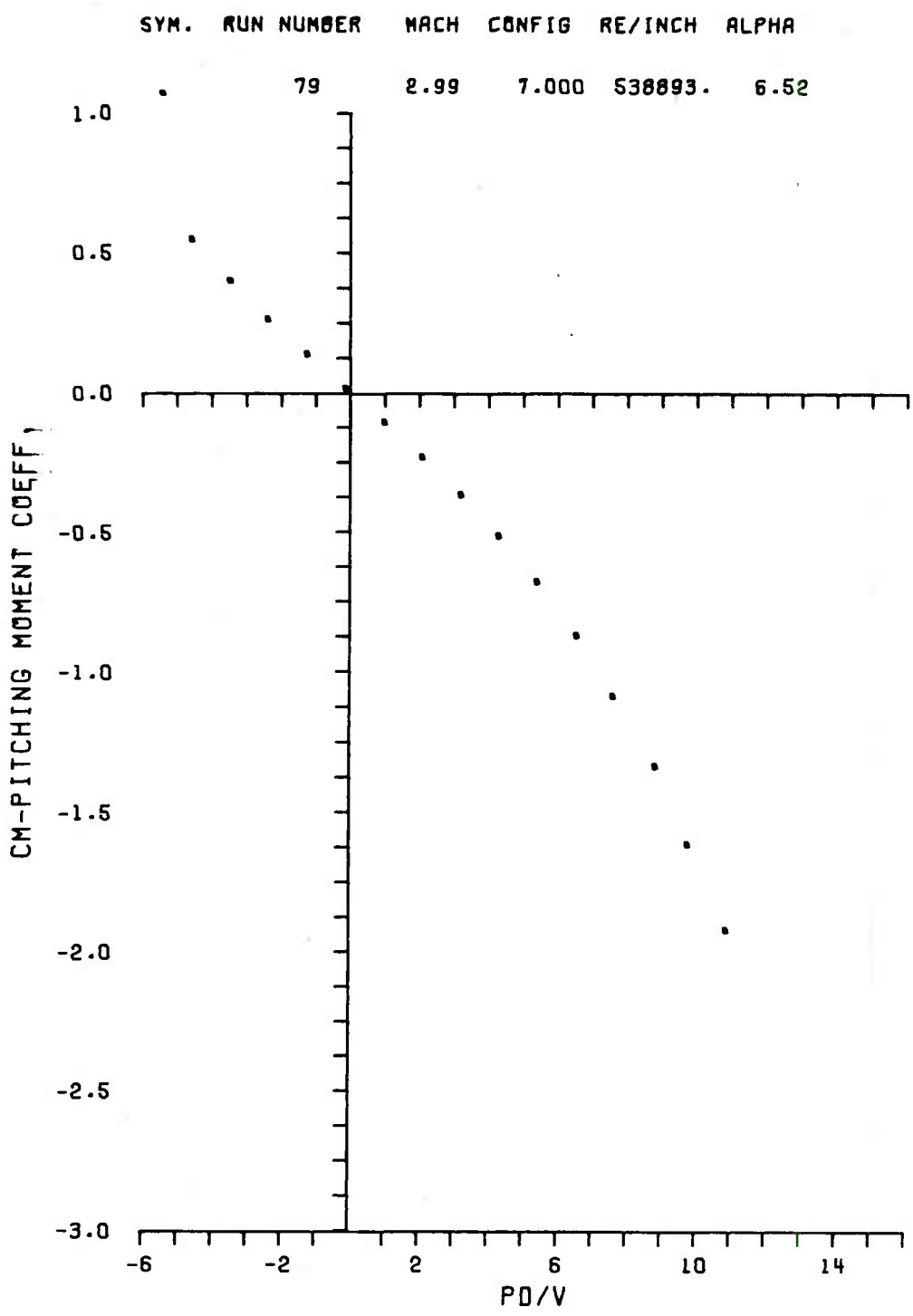

Figure B2. Continued

b. Tangent-Ogive-Cylinder with Boattail

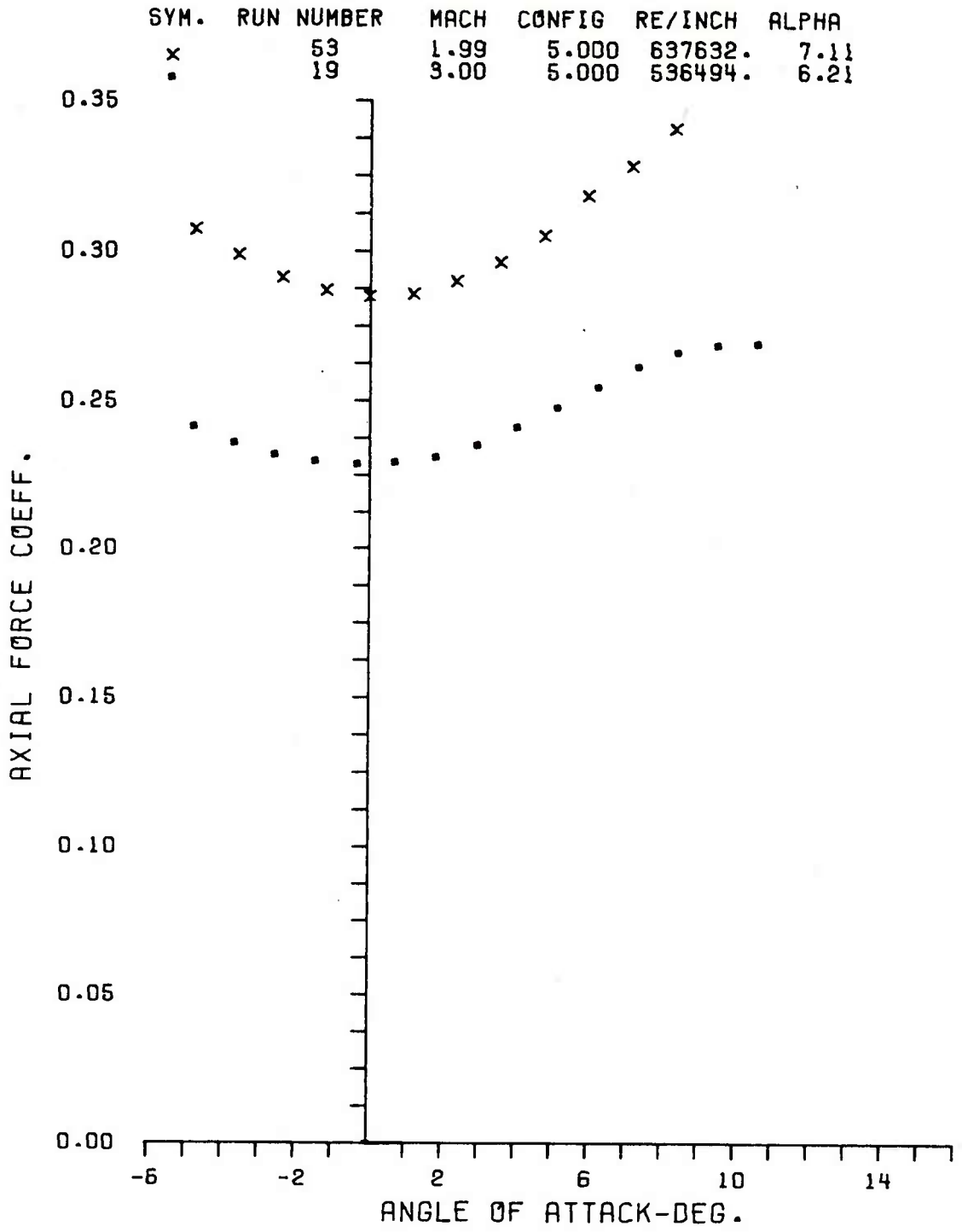

Figure B3. Axial Force Coefficient, C_A, Versus Angle of Attack

a. Tangent-Ogive-Cylinder

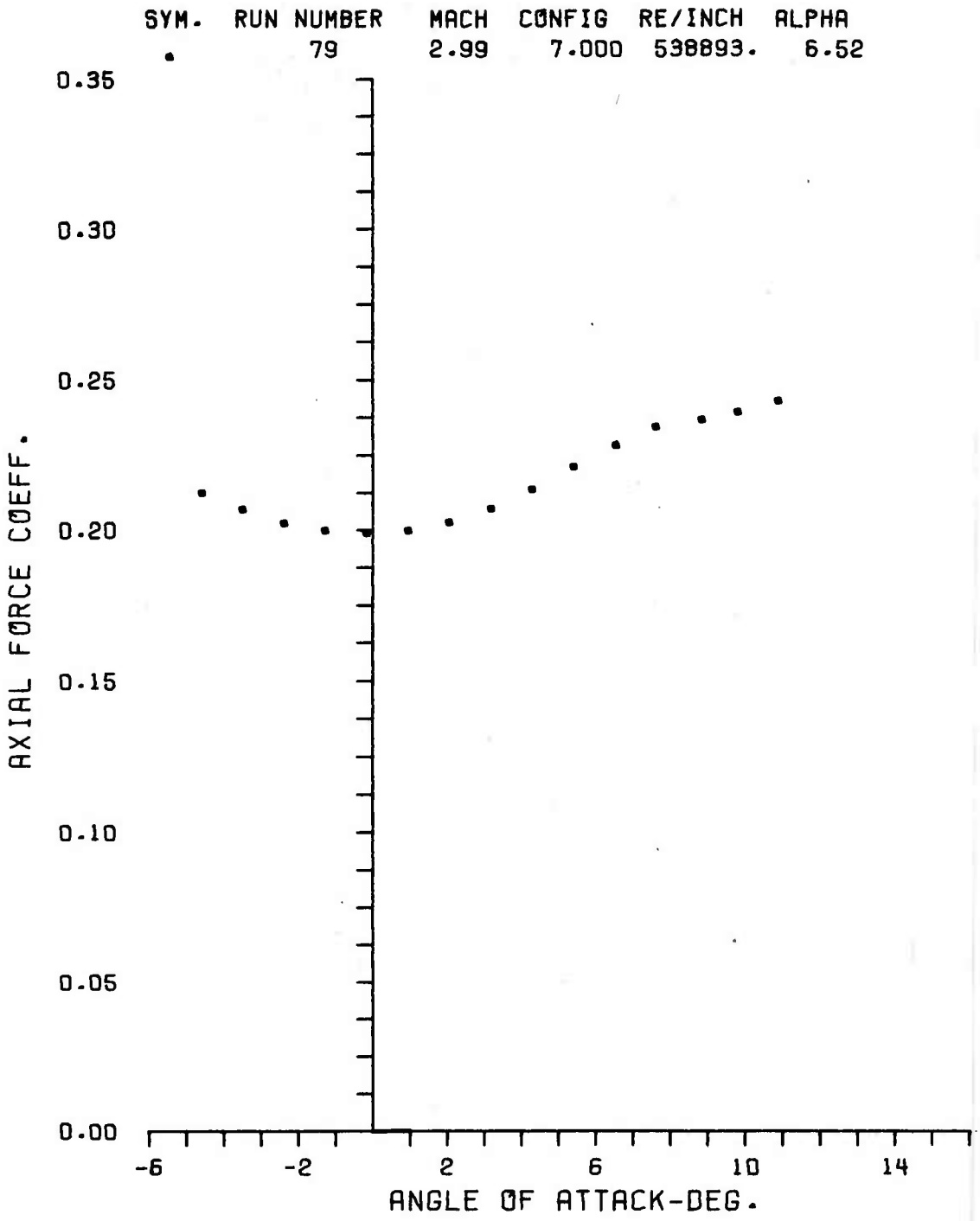

Figure B3. Continued

b. Tangent-Ogive-Cylinder with Boattail

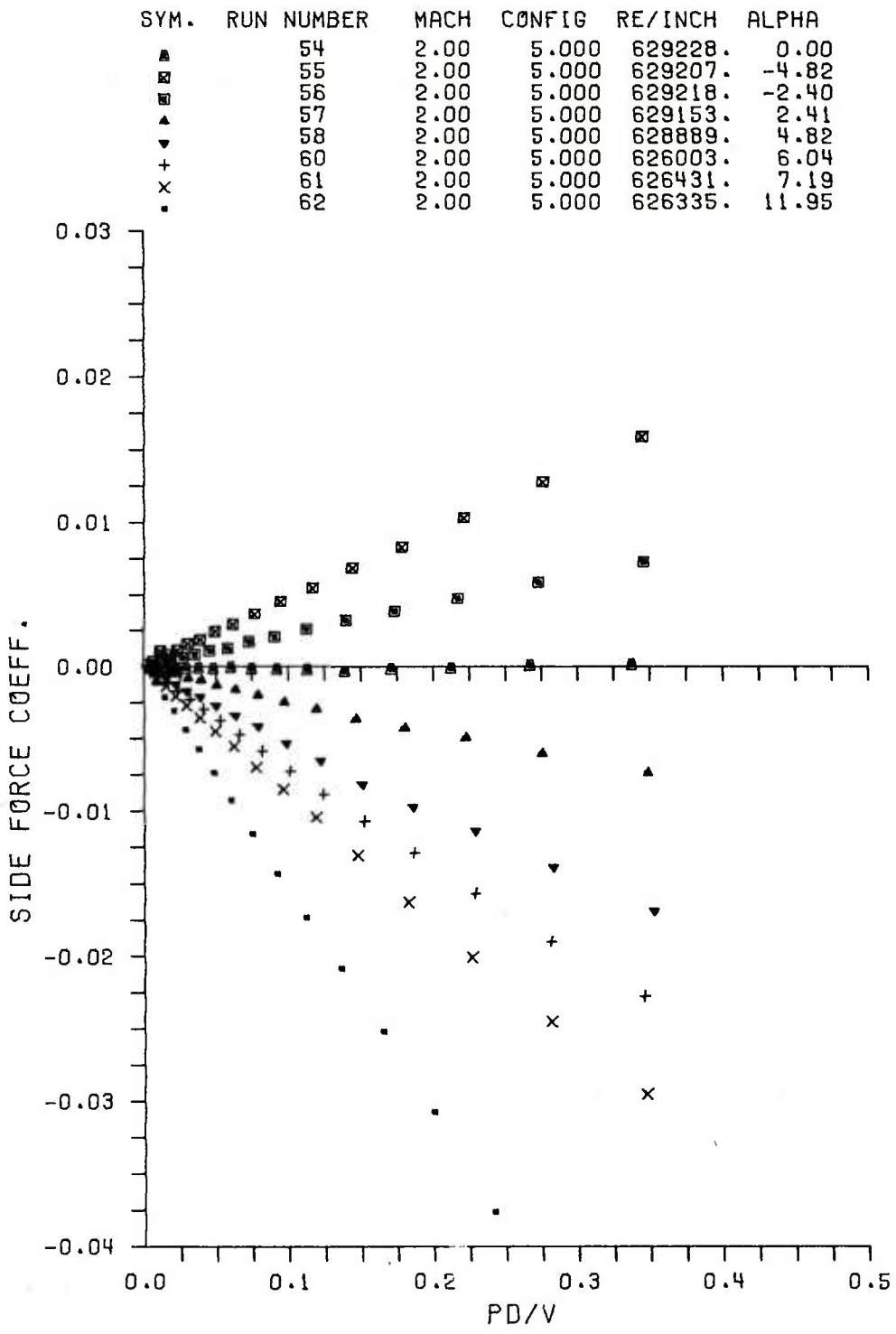

Figure B4. Side Force Coefficient, C_Y, Versus Spin Rate, Pd/V - Tangent-Ogive-Cylinder

a. M = 2.0

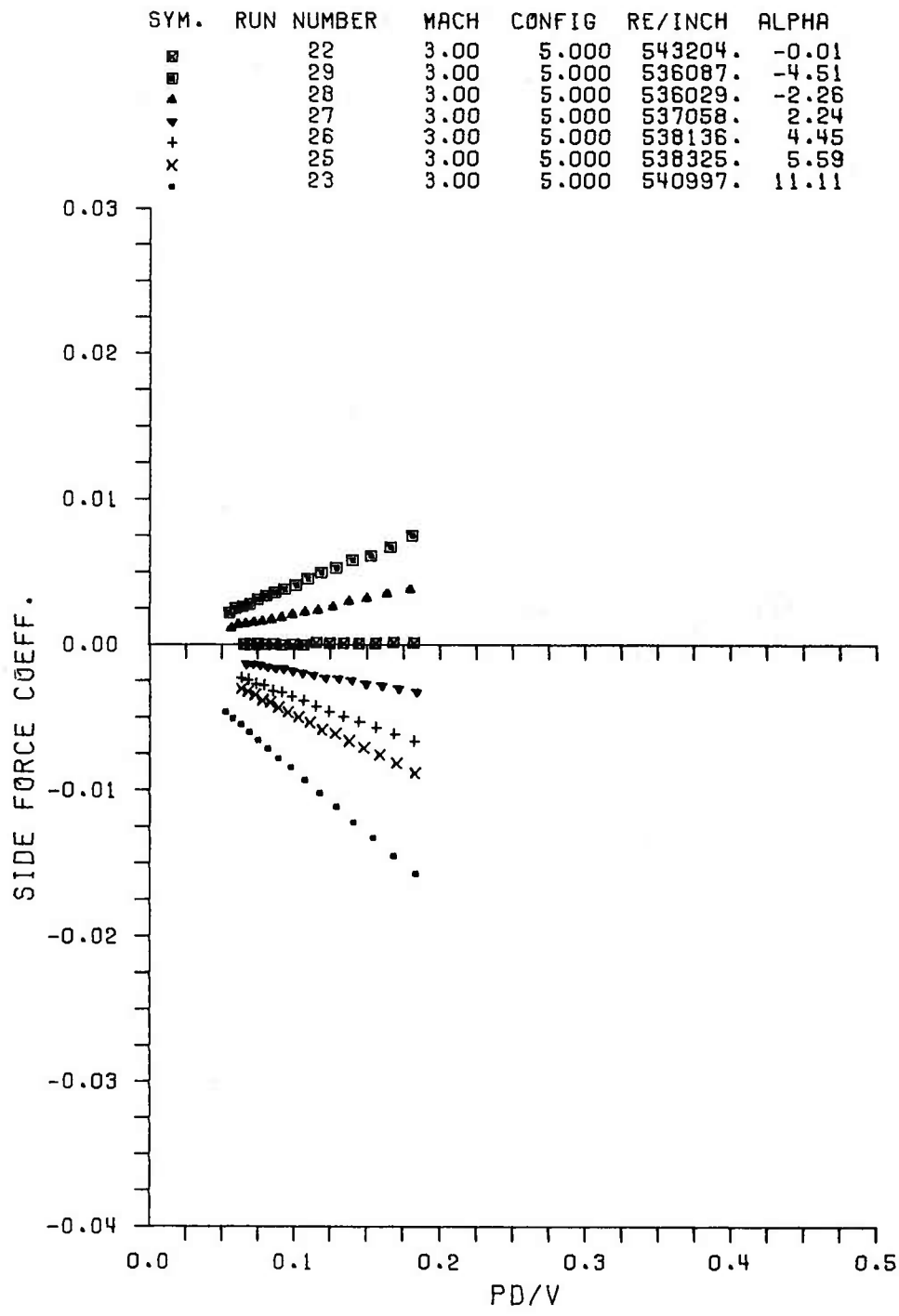

Figure B4. Continued

b. M = 3.0

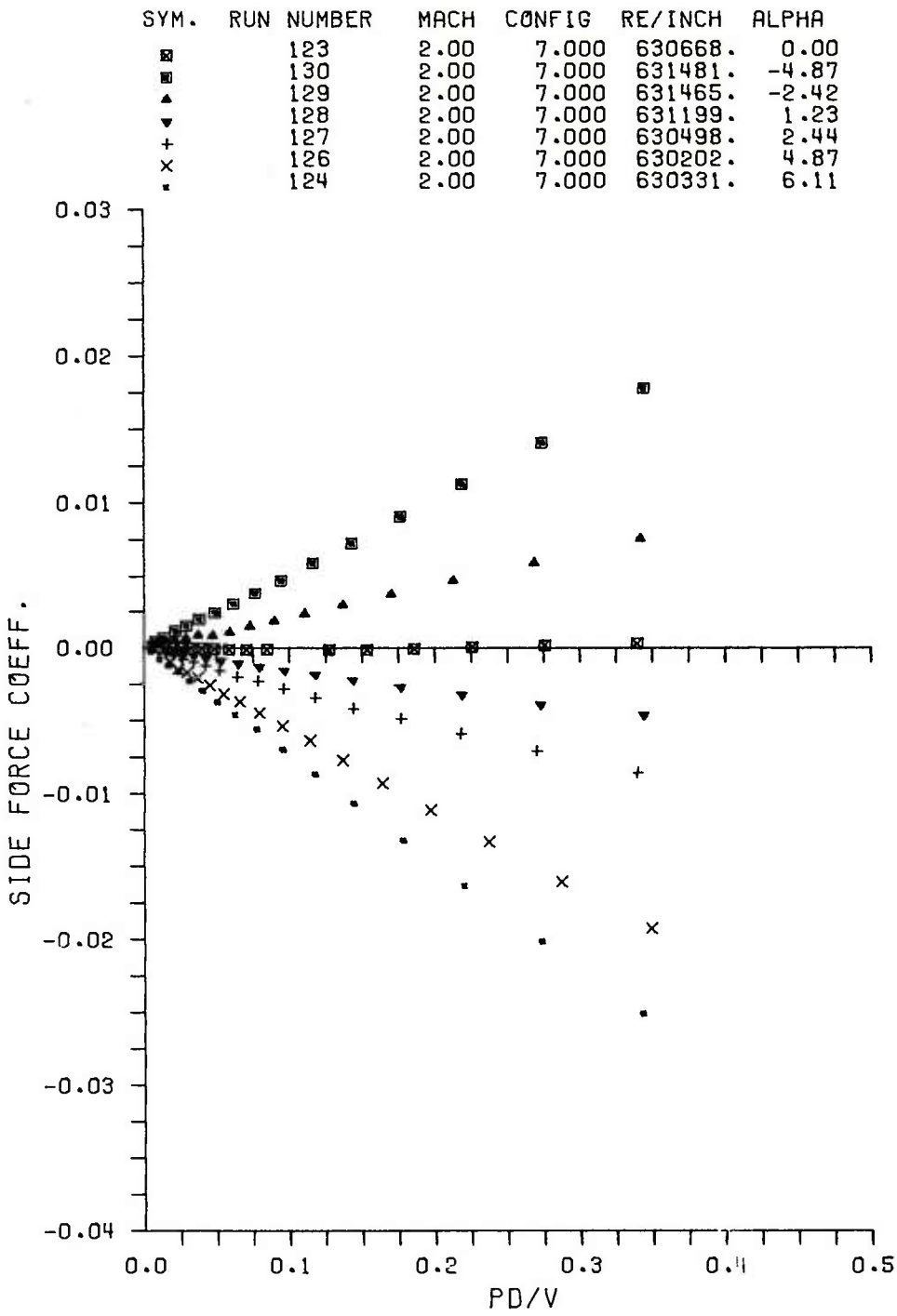

Figure B5. Side Force Coefficient, C_Y, Versus Spin Rate, Pd/V - Tangent-Ogive-Cylinder with Boattail

a. M = 2.0

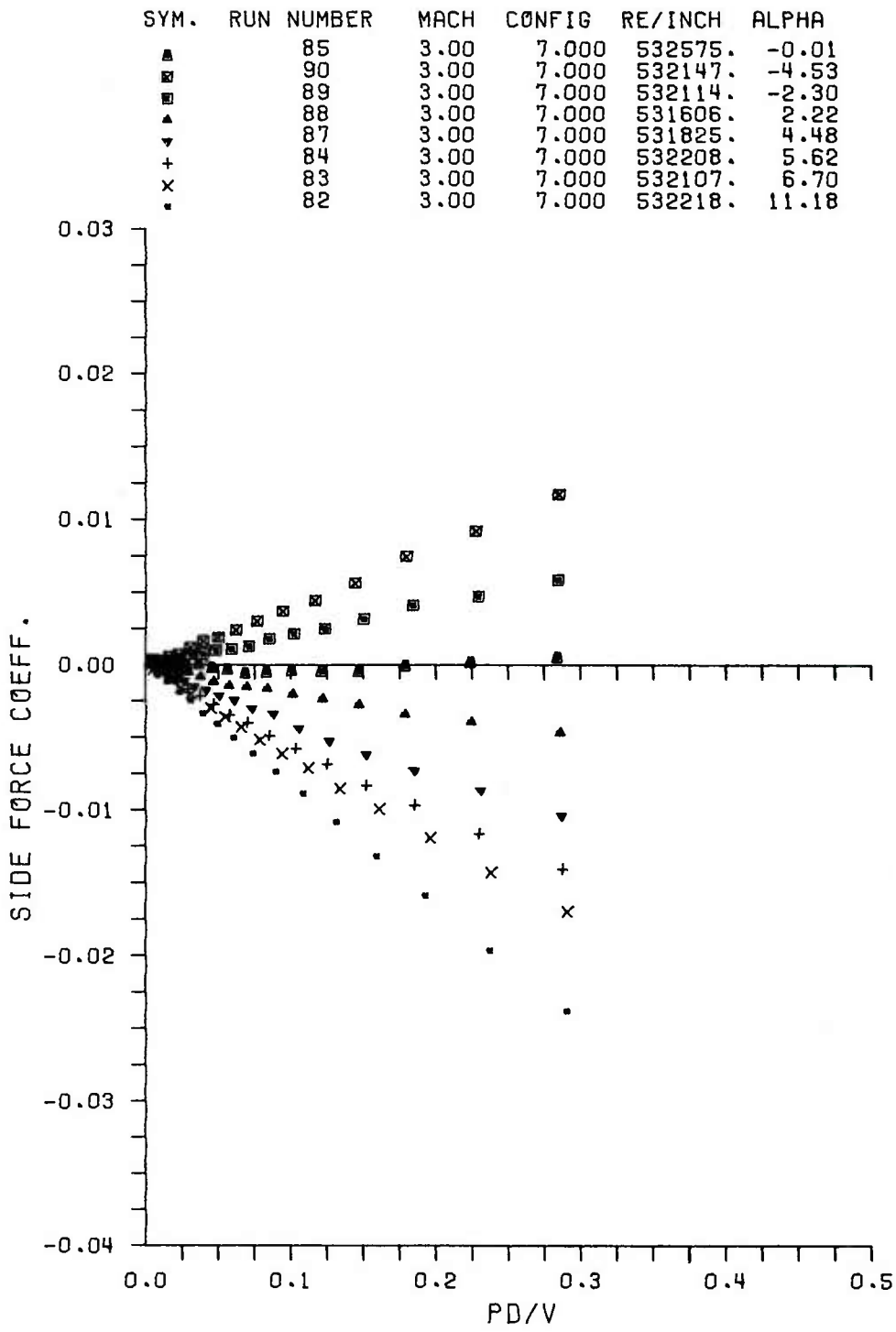

Figure B5. Continued

b. M = 3.0

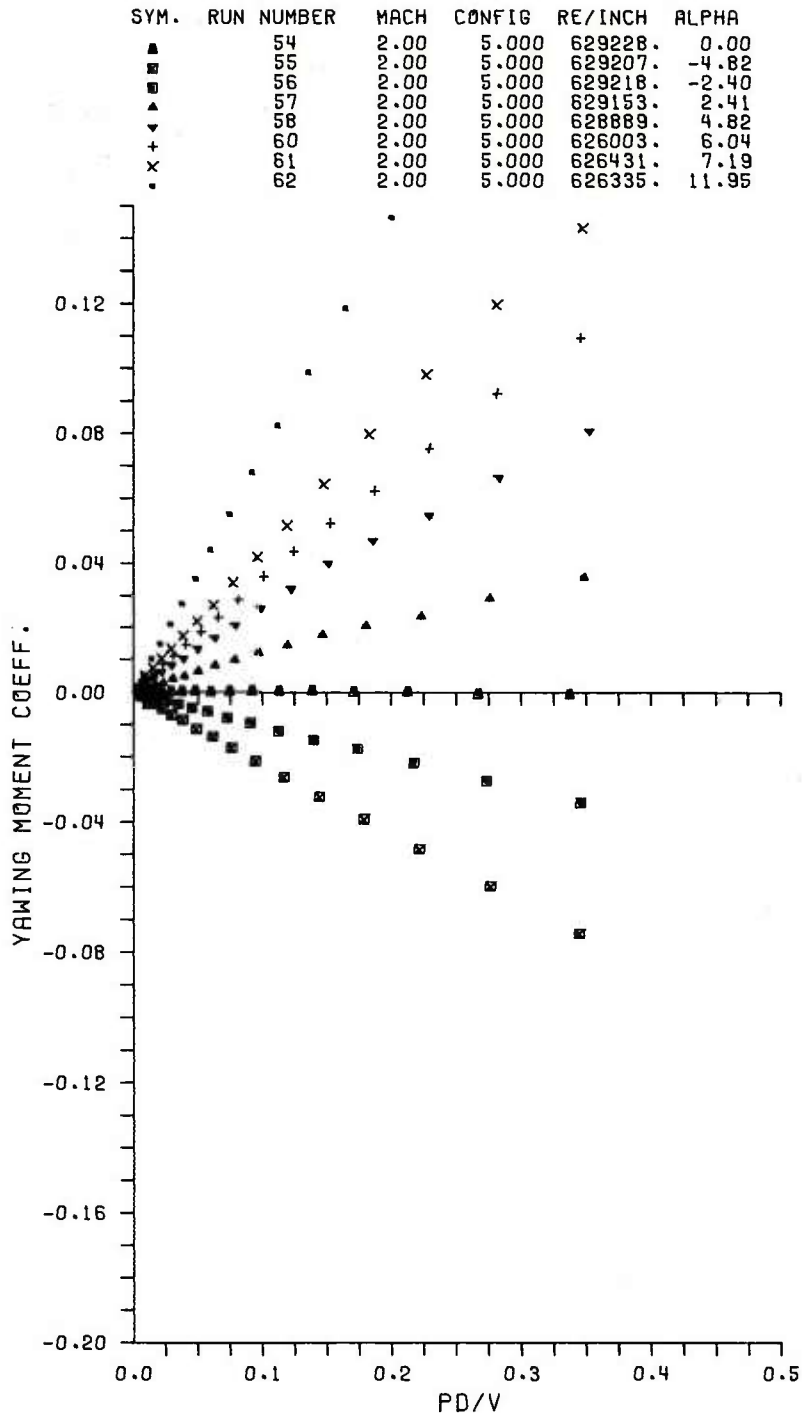

Figure B6. Yawing Moment Coefficient, C_n, Versus Spin Rate, Pd/V - Tangent-Ogive-Cylinder

a. M = 2.0

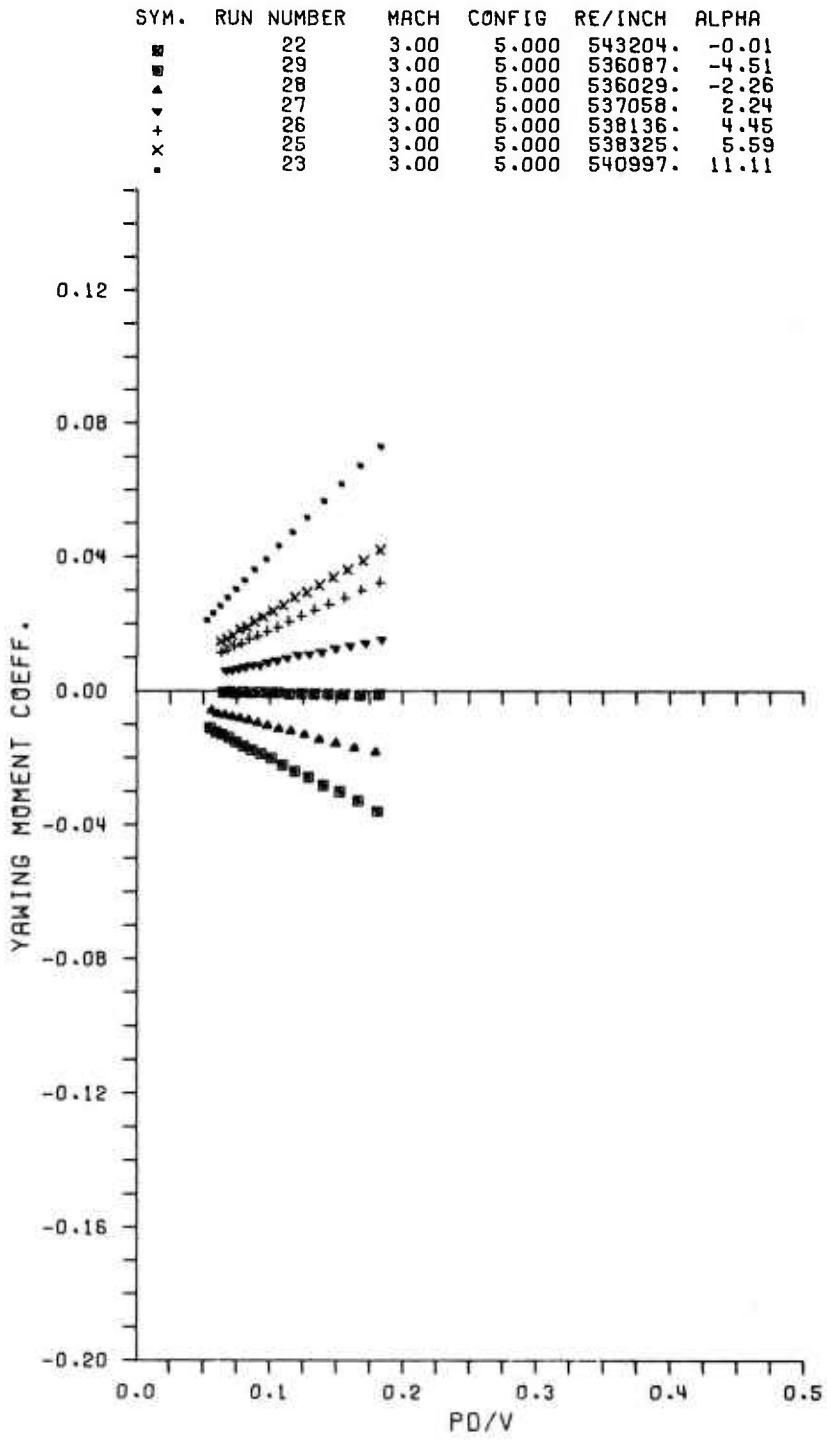

Figure B6. Continued

b. M = 3.0

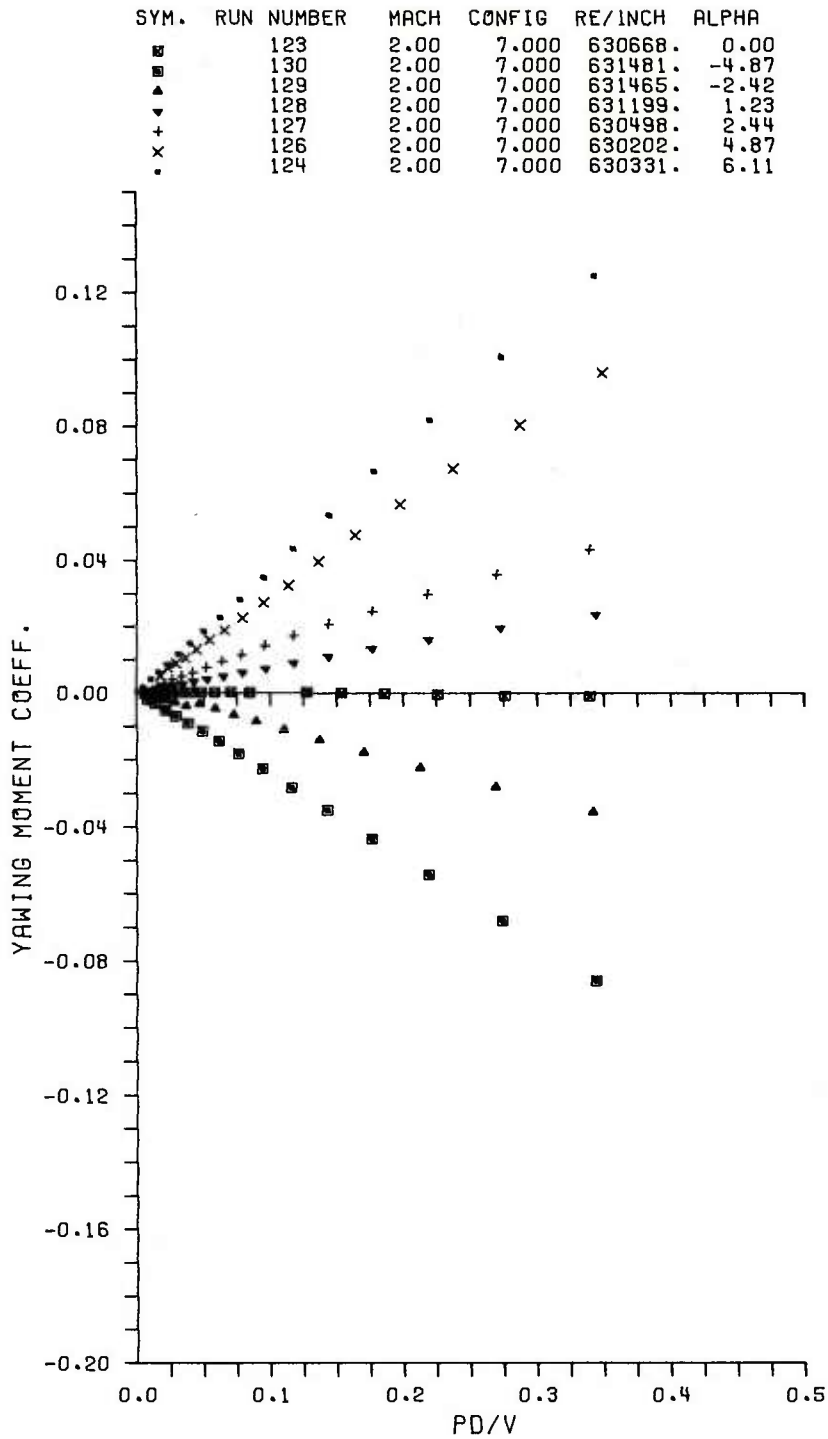

Figure B7. Yawing Moment Coefficient, C_n, Versus Spin Rate, Pd/V - Tangent-Ogive-Cylinder with Boattail

a. M = 2.0

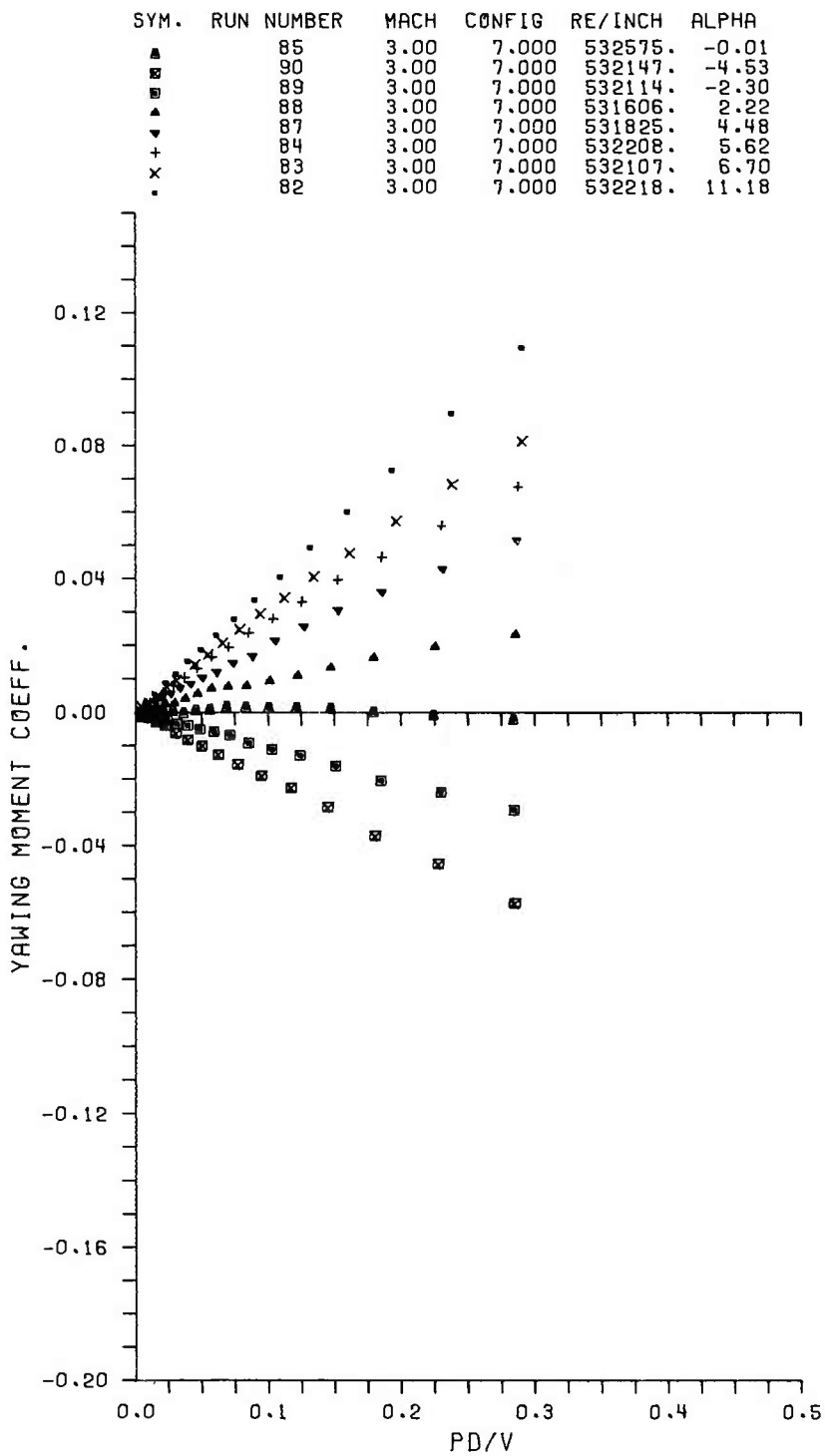

Figure B7. Continued

b. M = 3.0

DISTRIBUTION LIST

No. of Copies	Organization
12	Commander Defense Technical Info Center ATTN: DDC-DDA Cameron Station Alexandria, VA 22314
1	Commander US Army Materiel Development and Readiness Command ATTN: DRCDMD-ST 5001 Eisenhower Avenue Alexandria, VA 22333
8	Commander US Army Armament Research & Development Command ATTN: DRDAR-TSS (2 cys) DRDAR-LCA-F Mr. D. Mertz Mr. E. Falkowski Mr. A. Loeb Mr. R. Kline Mr. S. Kahn Mr. S. Wasserman Dover, NJ 07801
1	Commander US Army Armament Materiel Readiness Command ATTN: DRSAR-LEP-L, Tech Lib Rock Island, IL 61299
1	Director US Army ARRADCOM Benet Weapons Laboratory ATTN: DRDAR-LCB-TL Watervliet, NY 12189
1	Commander US Army Aviation Research & Developlment Command ATTN: DRSAV-E P.O. Box 209 St. Louis, MO 61366
1	Director US Army Air Mobility Research and Development Command Ames Research Center Moffett Field, CA 94035
1	Commander US Army Communications Research & Development Command ATTN: DRDCO-PPA- SA Fort Monmouth, NJ 07703
1	Commander US Army Electronics Research & Development Command Technical Support Activity ATTN: DELSD-L Fort Monmouth, NJ 07703
4	Commander US Army Missile Command ATTN: DRSMI-R DRSMI-YDL DRSMI-RDK Mr. R. Deep Mr. R. Becht Redstone Arsenal, AL 35809
1	Commander US Army Tank Automotive Research & Development Command ATTN: DRDTA-UL Warren, MI 48090
1	Commander US Army Research Office P.O. Box 12211 Research Triangle Park NC 27709
1	Director US Army TRADOC Systems Ananlysis Activity ATTN: ATAA-SL, Tech Lib White Sands Missile Range NM 88002

DISTRIBUTION LIST

No. of Copies	Organization
1	Commander Naval Air Systems Command ATTN: AIR-604 Washington, DC 20360
2	Commander David W. Taylor Naval Ship Research & Development Ctr ATTN: Dr. S. de los Santos Mr. Stanley Gottlieb Bethesda, Maryland 20084
4	Commander Naval Surface Weapons Center ATTN: Dr. T. Clare, Code DK20 Dr. P. Daniels Mr. D.A. Jones III Mr. L. Mason Dahlgren, VA 22448
3	Commander Naval Surface Weapons Center ATTN: Code 312 Mr. F. Regan Mr. J. Knott Mr. R. Schlie Silver Spring, MD 20910
1	Commander Naval Weapons Center ATTN: Technical Library China Lake, CA 93555
2	Director NASA Ames Research Center ATTN: MS-202, Tech Lib MS-227-8, Dr. L.B. Schiff Moffett Field, CA 94035
1	Director NASA Langley Research Center ATTN: MS-185, Tech Lib Langley Station Hampton, VA 23365
1	Arnold Research Organization, INc. von Karman Gas Dynamics Facility ATTN: Dr. John C. Adams, Jr. Aerodynamics Division Projects Branch Arnold AFS, TN 37389
1	Flow Simulations, Inc. ATTN: Dr. J. Steger 735 Alice Avenue Mountain View, CA 94041
1	Sandia Laboratories ATTN: Division No. 1331 Mr. H.R. Vaughn P.O. Box 580 Albuquerque, NM 87115
2	Massachusetts Institute of Technology ATTN: Prof. E. Covert Prof. C. Haldeman 77 Massachusetts Avenue Cambridge, MA 02139
1	Virginia Polytechnic Institute and State University Department of Aerospace and Ocean Engineering ATTN: Prof. George R. Inger Blacksburg, VA 24061
1	University of Delaware Mechanical and Aerospace Engineering Department ATTN: Dr. James E. Danberg Newark, DE 19711

DISTRIBUTION LIST

Organization

Aberdeen Proving Ground

Director, USAMSAA
ATTN: DRXSY-D
DRXSY-MP, H. Cohen

Cdr, USATECOM
ATTN: DRSTE-TO-F

Dir, Wpns Sys Concepts Team
Bldg E3516, EA
ATTN: DRDAR-ACW
Mr. M. Miller
Mr. A. Flatau

Dir, CSL
Bldg. E3160, EA
ATTN: Dr. W. Sacco

USER EVALUATION OF REPORT

Please take a few minutes to answer the questions below; tear out this sheet and return it to Director, US Army Ballistic Research Laboratory, ARRADCOM, ATTN: DRDAR-TSB, Aberdeen Proving Ground, Maryland 21005. Your comments will provide us with information for improving future reports.

1. BRL Report Number _____

2. Does this report satisfy a need? (Comment on purpose, related project, or other area of interest for which report will be used.)

_____

_____

_____

3. How, specifically, is the report being used? (Information source, design data or procedure, management procedure, source of ideas, etc.) _____

_____

_____

4. Has the information in this report led to any quantitative savings as far as man-hours/contract dollars saved, operating costs avoided, efficiencies achieved, etc.? If so, please elaborate.

_____

_____

5. General Comments (Indicate what you think should be changed to make this report and future reports of this type more responsive to your needs, more usable, improve readability, etc.) _____

_____

_____

_____

6. If you would like to be contacted by the personnel who prepared this report to raise specific questions or discuss the topic, please fill in the following information.

Name: _____

Telephone Number: _____

Organization Address: _____

_____

_____